



Transportation Research Division



Technical Report 15-06

*Experimental Evaluation and Design of
Unfilled and Concrete-Filled FRP
Composite Piles*

Task 1 - Mechanical Properties of FRP Piles

Final Report – Task 1, October 2015

Technical Report Documentation Page

1. Report No. ME 15-06	2.	3. Recipient's Accession No.	
4. Title and Subtitle Experimental Evaluation and Design of Unfilled and Concrete-Filled FRP Composite Piles Task 1 - Mechanical Properties of FRP Piles		5. Report Date October 2014	
		6.	
7. Author(s) Dale Lawrence Roberto Lopez-Anido Thomas Sandford Keenan Goslin Xenia Rofes		8. Performing Organization Report No. AEWC Report Number 15-9-1199	
9. Performing Organization Name and Address University of Maine – Advanced Structures and Composites Center		10. Project/Task/Work Unit No.	
		11. Contract © or Grant (G) No. Contract # 20130731*535	
12. Sponsoring Organization Name and Address Maine Department of Transportation		13. Type of Report and Period Covered	
		14. Sponsoring Agency Code	
15. Supplementary Notes			
16. Abstract (Limit 200 words) <p>The overall goal of this project is the experimental evaluation and design of unfilled and concrete-filled FRP composite piles for load-bearing in bridges. This report covers Task 1, Mechanical Properties of FRP Piles.</p> <p>Mechanical and geotechnical properties of fiber reinforced polymer (FRP) piles driven at the Richmond-Dresden Bridge Site (Maine DOT PIN 12674) in August 2013 were determined using coupon level tests. These properties will be used to evaluate the behavior of FRP piles in load bearing applications.</p>			
17. Document Analysis/Descriptors Bridge piles, fiber reinforced polymer composites, mechanical properties		18. Availability Statement	
19. Security Class (this report)	20. Security Class (this page)	21. No. of Pages 85	22. Price



Technical Report

Mechanical Properties of FRP Piles

by

**Dale Lawrence, Roberto Lopez-Anido¹, Thomas Sandford,
Keenan Goslin and Xenia Rofes**

**Project: Experimental Evaluation and Design of Unfilled and
Concrete-Filled FRP Composite Piles**

**Prepared for:
Dale Peabody P.E.
Director of Transportation Research
Maine Dept. of Transportation
16 State House Station
Augusta, Maine 04333**

**October 9th, 2014
UMaine's Advanced Structures and Composites Center
Project Number 15-9-1199**

¹ Department of Civil and Environmental Engineering, University of Maine
rla@maine.edu Phone: (207) 581-2119

Table of Contents

1. EXECUTIVE SUMMARY 3

2. REFERENCES 4

3. INTRODUCTION 5

4. MATERIALS AND SAMPLE DESCRIPTION..... 5

5. DATA ANALYSIS 6

6. TENSION 6

7. COMPRESSION 8

8. SHEAR 10

9. GLASS TRANSITION TEMPERATURE..... 12

10. SOIL-FRP FRICTION 15

 10.1. GRAIN SIZE ANALYSIS 15

 10.2. SPECIFIC GRAVITY 17

 10.3. MAXIMUM AND MINIMUM DENSITY 17

 10.4. ATTERBERG LIMITS 19

 10.5. DIRECT SHEAR (SOIL-SOIL) 20

 10.6. INTERFACE FRICTION (SOIL-FRP)..... 21

11. DISCUSSION 22

12. CONCLUSIONS 23

APPENDIX A: TENSION RESULTS 26

APPENDIX B: COMPRESSION RESULTS 33

APPENDIX C: SHEAR RESULTS 40

APPENDIX D: GLASS TRANSITION TEMPERATURE RESULTS 45

APPENDIX E: DIRECT SHEAR RESULTS 50

APPENDIX F: INTERFACE FRICTION RESULTS 68

1. Executive Summary

Representative fiber reinforced polymer (FRP) plates were tested at the coupon level to determine mechanical and geotechnical properties of FRP piles driven at the Richmond-Dresden bridge site in August 2013. Samples were tested in tension, compression, and shear. The resulting properties are presented in Table 1.

Table 1: Summary of Average Mechanical Properties of FRP Plates

Test	Orientation of Properties	Ultimate Strength (ksi)	Ultimate Strain (Microstrain)	Modulus (ksi)	Poisson's Ratio
Longitudinal Tension	X	76.9	2.56E+04	3.26E+03	0.31 (ν_{xy})
Hoop Tension	Y	25.3	2.27E+04	1.98E+03	–
Longitudinal Compression	X	72.0	-2.17E+04	3.67E+03	–
Hoop Compression	Y	34.7	-1.65E+04	2.14E+03	–
In-Plane Shear	XY	22.3	2.88E+04	8.49E+02	–

The glass transition temperature was also determined using dynamic mechanical analysis. The resulting properties are presented in Table 2.

Table 2: Summary of Glass Transition Temperatures

Indicator of Glass Transition Temperature	Glass Transition Temperature (°C)
Onset Point of Storage Modulus	81.0
Peak of Loss Modulus	94.8
Peak of Tan Delta	116.6

Testing was conducted to determine the interface friction angle between the FRP plates and 3 soils. The resulting properties are presented in Table 3.

Table 3: Summary of Friction Testing

Sample		Direct Shear		Interface Friction	
Soil	Density	Peak (Degrees)	Constant Volume (Degrees)	Peak (Degrees)	Constant Volume (Degrees)
Ottawa Sand	Medium Dense	36.4	31.5	28.2	26.3
	Dense	39.1	34.5	32.6	27.3
MDOT Backfill	Medium Dense	40.9	39.1	28.4	28.2
	Dense	42.1	35.3	31.8	28.9
Glacial Till	Medium Dense	39.4	38.4	31.6	30.9
	Dense	40.7	38.7	32.3	32.1

2. References

ASTM D3039-08 Tensile Properties of Polymer Matrix Composite Materials

ASTM D6641-09 Compressive Properties of Polymer Matrix Composite Materials Using a Combined Loading Compression (CLC) Test Fixture

ASTM D7078-12 Shear Properties of Composite Materials by V-Notched Rail Shear Method

ASTM E 1640-09 Assignment of the Glass Transition Temperature by Dynamic Mechanical Analysis

TS-64: Measurement of the Glass Transition Temperature Using Dynamic Mechanical Analysis. Thermal Analysis Instruments

ASTM D6913-04 (Reapproved 2009) Particle-Size Distribution (Gradation) of Soils Using Sieve Analysis

ASTM D854-10 Specific Gravity of Soil Solids by Water Pycnometer

ASTM D4253-00 (Reapproved 2006) Maximum Index Density and Unit Weight of Soils Using a Vibratory Table

ASTM D4254-00 (Reapproved 2006) Minimum Index Density and Unit Weight of Soils and Calculation of Relative Density

ASTM D4318-10 Liquid Limit, Plastic Limit, and Plasticity Index of Soils

ASTM D3080-11 Direct Shear Test of Soils Under Consolidated Drained Conditions

3. Introduction

Mechanical and geotechnical properties of fiber reinforced polymer (FRP) piles driven at the Richmond-Dresden Bridge Site (Maine DOT PIN 12674) in August 2013 were determined using coupon level tests. These properties will be used to evaluate the behavior of FRP piles in load bearing applications. The following tests were conducted to determine material properties:

- Tension (ASTM D3039)
- Compression (ASTM D6641)
- Shear (ASTM D7078)
- Glass Transition Temperature (ASTM E1640)
- Interface Friction (Modified ASTM D3080)

4. Materials and Sample Description

Coupons for material testing were cut from FRP plates provided by Harbor Technologies, LLC. All plates were manufactured using two layers of stitched E-glass fabric with reinforcing fibers in the 0, 90, and +/- 45 degree orientation and a polyester resin. Both layers of reinforcement have the zero degree fibers facing the gel coat, which creates an un-symmetric but balanced laminate. Upon delivery to the Advanced Structures and Composites Center, the consolidated plates were warped. This is likely a result of thermal stresses during the curing process and the un-symmetric stacking sequence of the lamina.

All coupons were cut using a Flow Mach4 4020b abrasive cutting machine to the dimensions specified in their corresponding ASTM standard. After cutting, all coupons were conditioned at 73 degrees Fahrenheit and 50% relative humidity for a minimum of 3 days prior to testing. Testing was conducted using an Instron 8801 test frame and Instron Dynacell +/- 100 kN load cell. ARAMIS digital image correlation software was used to measure strains during all coupon tests requiring strain measurement.

Tension, compression, and shear coupons were all tested in the longitudinal and hoop direction. The terms longitudinal and hoop refer to the orientation of the 0 degree fibers and also coincides with the longitudinal and hoop direction of the full scale FRP piles. This is presented graphically in Figure 1.

The longitudinal direction corresponds to the x-axis and the hoop direction corresponds to the y-axis.

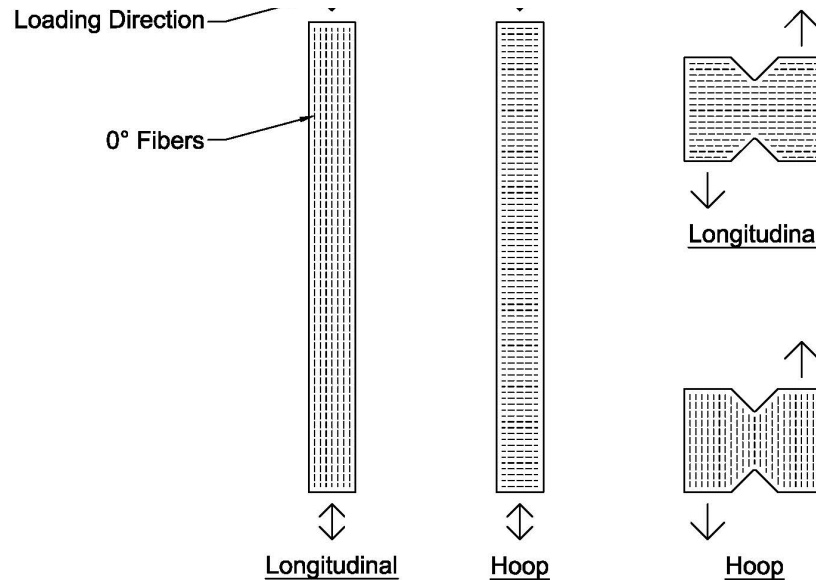


Figure 1: Fiber Orientation of Coupon Samples

5. Data Analysis

Modulus of elasticity, Poisson's ratio, and shear modulus were calculated over the same strain range for all samples. The strain range of 3,000 to 10,000 microstrain was determined to be a linear range shared by all tests. Calculations were conducted using the chord method and a linear regression over the same strain range.

6. Tension

All tensile testing was conducted in accordance with ASTM D3039. Twelve tension coupons were tested in the longitudinal and hoop orientation.

Some longitudinal tension samples slipped in the grips during testing with a maximum available gripping pressure of approximately 2500 psi. Grit paper was added to the grips of the Instron testing machine to limit slipping of the sample during tests. Several longitudinal tension samples were discounted due to slipping in the grips. The test fixture can be seen in Figure 2.



Figure 2: Tension Coupon Test

Hoop tension samples showed a bi-linear stress-strain relationship. Elastic modulus and Poisson’s ratio were calculated using a strain range of 1000 to 3000 microstrain to capture the initial slope of the stress-strain curve. The results of longitudinal and hoop tension tests can be seen in Table 4.

Table 4: Tension Results

		Ultimate Stress (ksi)	Ultimate Strain (μstrain)	Modulus (ksi)	Poisson’s Ratio
Longitudinal Tension	Mean	76.9	2.56E+04	3.26E+03 (E_x)	0.31 (ν_{xy})
	Std. Dev.	1.6	9.85E+02	1.83E+02	0.04
	COV	2.14%	3.85%	2.37%	13.55%
Hoop Tension	Mean	25.3	2.27E+04	1.98E+03 (E_y)	0.14 (ν_{yx})
	Std. Dev.	1.1	1.10E+03	1.03+02	0.04
	COV	4.52%	4.86%	5.19%	26.19%

The reciprocity condition for the elastic properties obtained from the tensions tests was checked using (1). It was found that there was a difference of 32.5 percent between the left and right hand of the relationship.

$$\frac{v_{xy}}{E_x} = \frac{v_{yx}}{E_y} \tag{1}$$

Stress-strain plots of longitudinal and hoop tension tests can be seen in Figure 3 and Figure 4 respectively.

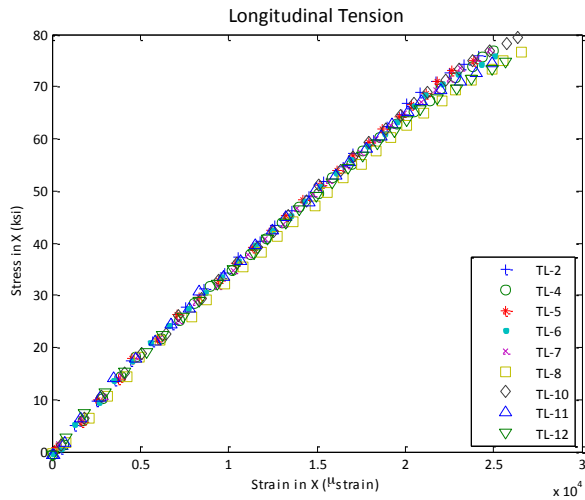


Figure 3: Stress vs. Strain of Longitudinal Tension Samples

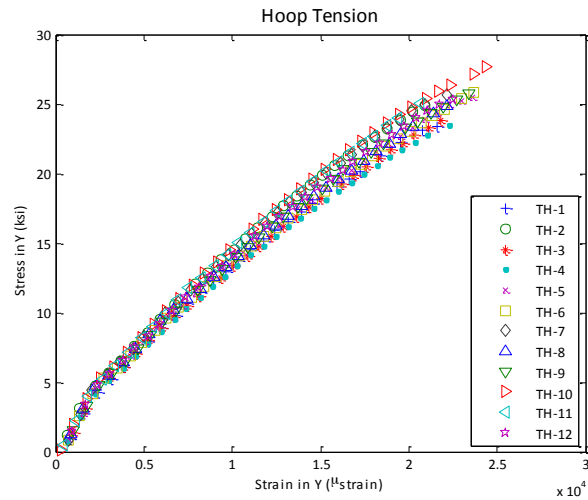


Figure 4: Stress vs. Strain of Hoop Tension Samples

Results of individual tension tests can be seen in Appendix A.

7. Compression

All compression testing was conducted in accordance with ASTM D6641. Twelve compression coupons were tested in the longitudinal and hoop orientation.

The ASTM standard for this test suggests a bolt torque of 20 to 25 inch-lbs. The bolt torque was increased to 50 inch-lbs to prevent samples from slipping in the test fixture. The test fixture can be seen in Figure 5.



Figure 5: Compression Coupon Test

The results of longitudinal and hoop compression tests can be seen in Table 5.

Table 5: Compression Results

		Ultimate Stress (ksi)	Ultimate Strain (μstrain)	Modulus (ksi)
Longitudinal Compression	Mean	72.0	-2.17E+04	3.67E+03 (E_x)
	Std. Dev.	5.0	2.90E+03	2.46E+02
	COV	6.99%	13.36%	6.70%
Hoop Compression	Mean	34.7	-1.65E+04	2.14E+03 (E_y)
	Std. Dev.	1.9	1.51E+03	7.25E+01
	COV	5.57%	9.12%	3.39%

Elastic properties E_x , E_y , and ν_{xy} are adopted from the tension tests.

Stress-strain plots of longitudinal and hoop compression tests can be seen in Figure 6 and Figure 7 respectively.

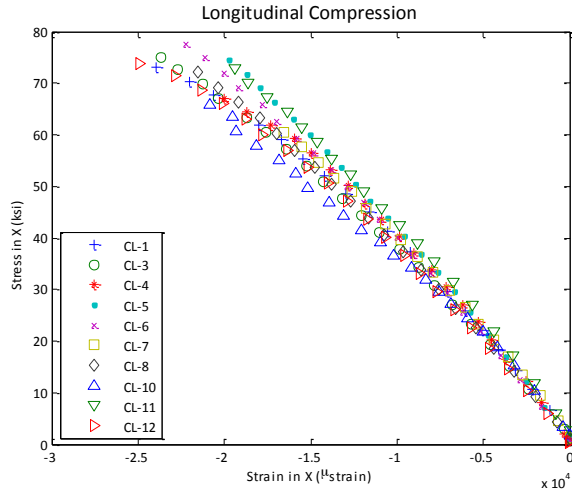


Figure 6: Stress vs. Strain of Longitudinal Compression Samples

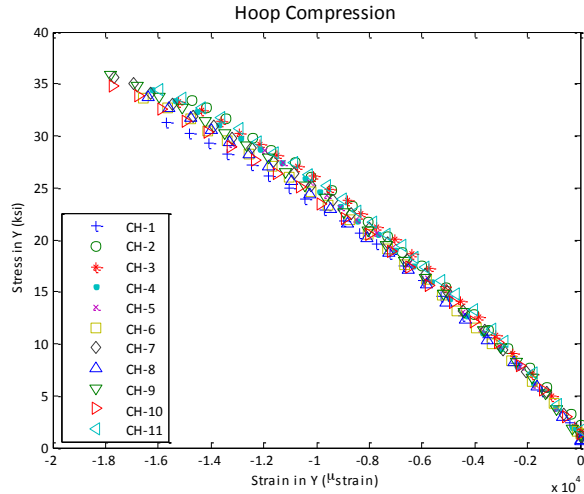


Figure 7: Stress vs. Strain of Hoop Compression Samples

Results of individual compression tests can be seen in Appendix B.

8. Shear

All shear testing was conducted in accordance with ASTM D7078. Twelve shear coupons were tested in the longitudinal and hoop orientation.

The ASTM standard used for this test was designed for samples with reinforcing only in the 0 and 90 degree directions. This material has reinforcing in the 0, 90, and +/- 45 degrees which gives the material a higher shear strength. The suggested bolt torque of 40 foot-lbs allowed samples to slip in the test fixture before failure, so the bolt torque was increased to 50 foot-lbs. The test fixture can be seen in Figure 8.

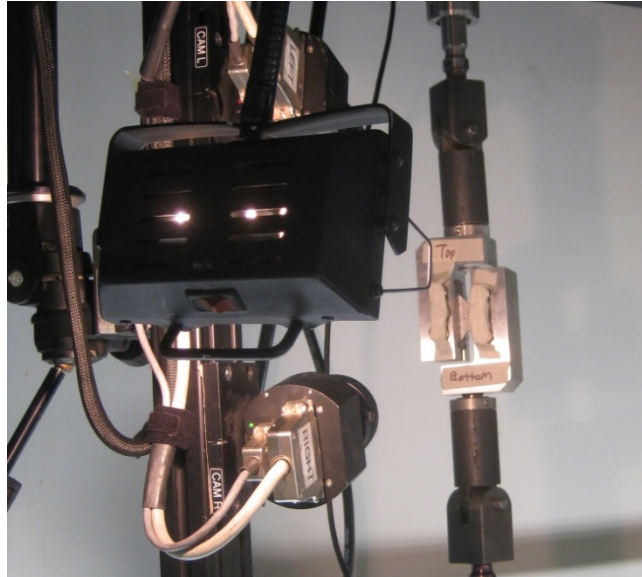


Figure 8: Shear Coupon Test

The results of longitudinal and hoop shear tests can be seen in Table 6.

Table 6: Shear Results

		Ultimate Stress (ksi)	Ultimate Strain (μstrain)	Modulus (ksi)
Longitudinal Loading	Mean	24.3	3.63E+04	8.94E+02 (G_{xy})
	Std. Dev.	1.4	3.86E+03	2.28E+01
	COV	5.57%	10.63%	2.55%
Hoop Loading	Mean	22.3	2.88E+04	8.49E+02 (G_{yx})
	Std. Dev.	2.1	4.23E+03	4.80E+01
	COV	9.63%	14.68%	5.65%

Stress-strain plots of longitudinal and hoop shear tests can be seen in Figure 9 and Figure 10 respectively.

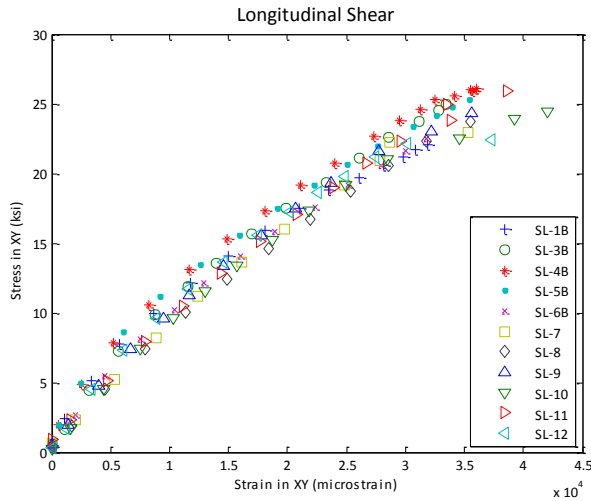


Figure 9: Stress vs. Strain of Longitudinal Shear Samples

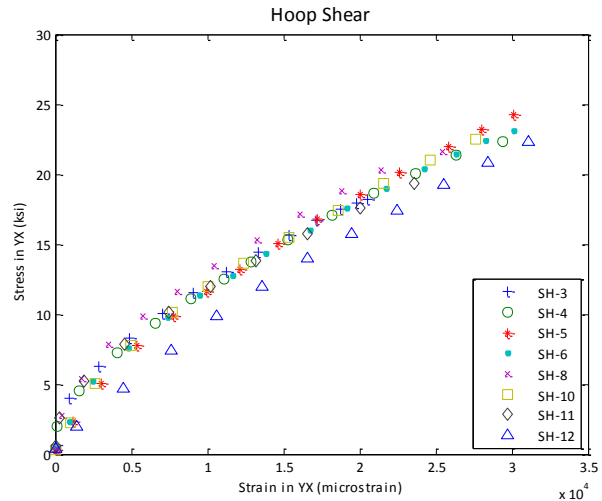


Figure 10: Stress vs. Strain of Hoop Shear Samples

Results of individual shear tests can be seen in Appendix C.

9. Glass Transition Temperature

Glass transition testing was conducted in accordance with ASTM E1640. A Thermal Analysis Instruments DMA Q800 dynamic mechanical analyzer was used to test samples. The 3 point bend test configuration was used to accommodate the thickness and modulus of the samples. The test set up can be seen in Figure 11.

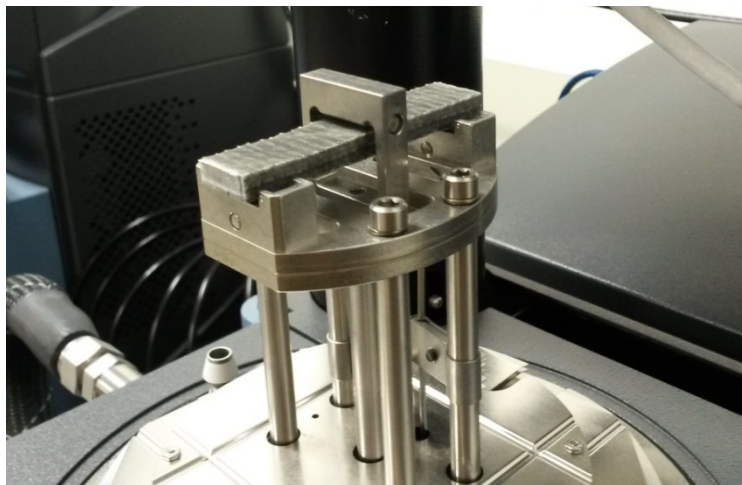


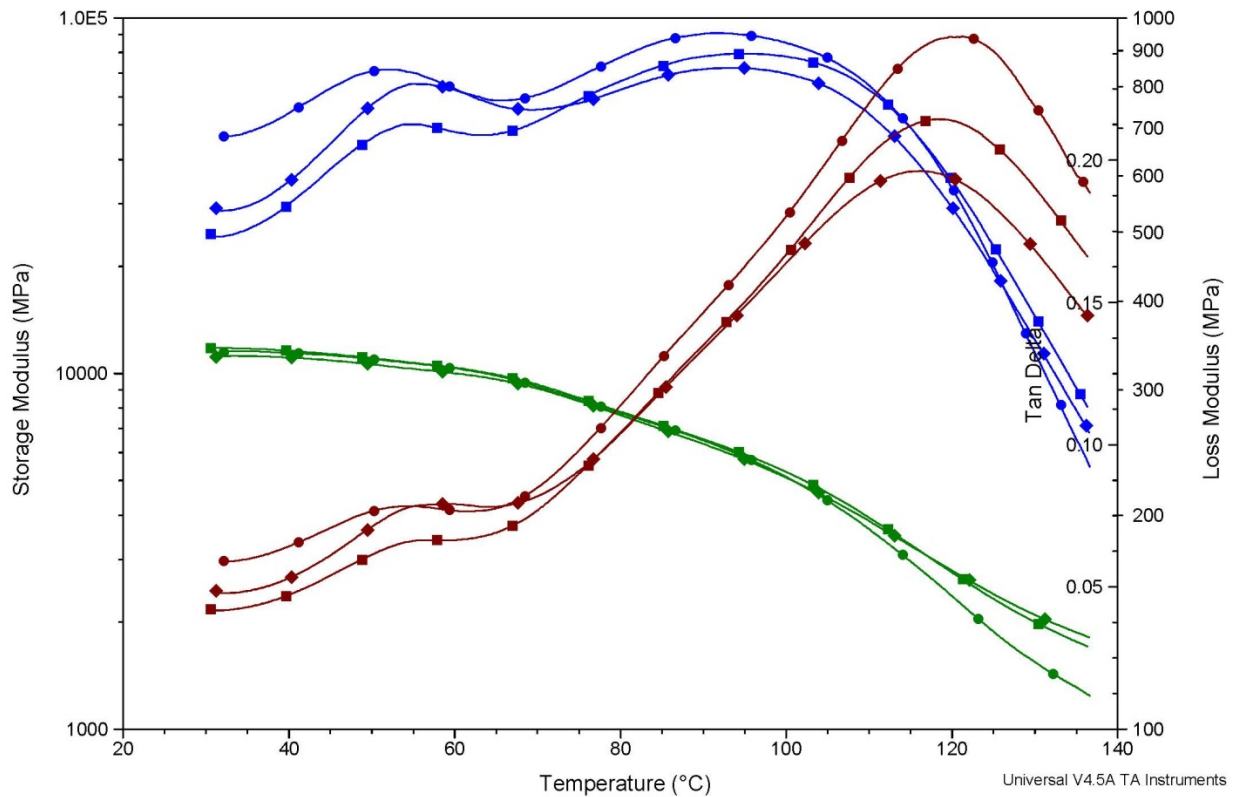
Figure 11: Glass Transition Test

Tests were run with a pre-load of 2 Newtons, frequency of 1 Hertz, temperature ramp of 3 degrees Centigrade per minute, and amplitude of 10 micrometers. Testing was conducted from 30 to 140 degrees Centigrade.

Dynamic mechanical analysis determines glass transition temperature using 3 properties. Thermal Analysis Instruments describes the 3 different glass transition temperatures as:

- Onset of the change in slope of storage modulus: “Occurs at the lowest temperature and relates to mechanical failure”
- Peak of the loss modulus: “Occurs at the middle temperature and is more closely related to the physical property changes attributed to the glass transition in plastics. It reflects molecular processes and agrees with the idea of T_g as the temperature at the onset of segmental motion”
- Tan Delta Peak: “Occurs at the highest temperature and is used historically in literature. It is a good measure of the ‘leather like’ midpoint between the glassy and rubbery states of a polymer. The height and shape of the tan delta peak change systematically with amorphous content”

For the purpose of this research, the onset of the change in slope of storage modulus will be used as the glass transition temperature in accordance with ASTM E1640.



A summary of the glass transition temperatures for each sample can be seen below in Table 7.

Table 7: Glass Transition Temperature Results

Sample	Onset Point of Storage Modulus (°C)	Peak of Loss Modulus (°C)	Peak of Tan Delta (°C)
Tg-1	80.6	93.2	118.2
Tg-2	83.9	96.5	116.9
Tg-3	78.6	94.7	114.8
Average	81.0	94.8	116.6

Results of individual glass transition temperature tests can be seen in Appendix D.

10. Soil-FRP Friction

Three soils were chosen for soil-FRP friction testing. These soils are: Ottawa sand, a backfill meeting Maine Department of Transportation (MaineDOT) specifications for Type B Aggregate, and a glacial till obtained from an excavation at the corner of Long Road and Rangeley Road in Orono, ME. All grains above the number 8 sieve were removed prior to all index and shear testing to meet the requirements of ASTM D3080 for the minimum sample height to maximum grain size ratio in direct shear tests.



Figure 12: Ottawa Sand



Figure 13: MDOT Backfill



Figure 14: Glacial Till

Prior to soil-FRP friction testing, a series of index tests were conducted to define each soil's properties.

10.1. Grain Size Analysis

Grain size analysis was performed on all soils in accordance with ASTM D6913. All soil tests were conducted on oven dry samples, and a wet sieve analysis was also conducted on the glacial till due to its high fines content. The sieve and shaker can be seen in Figure 15.



Figure 15: Sieve Shaker for Grain Size Analysis

The results of the grain size analysis can be seen in Figure 16.

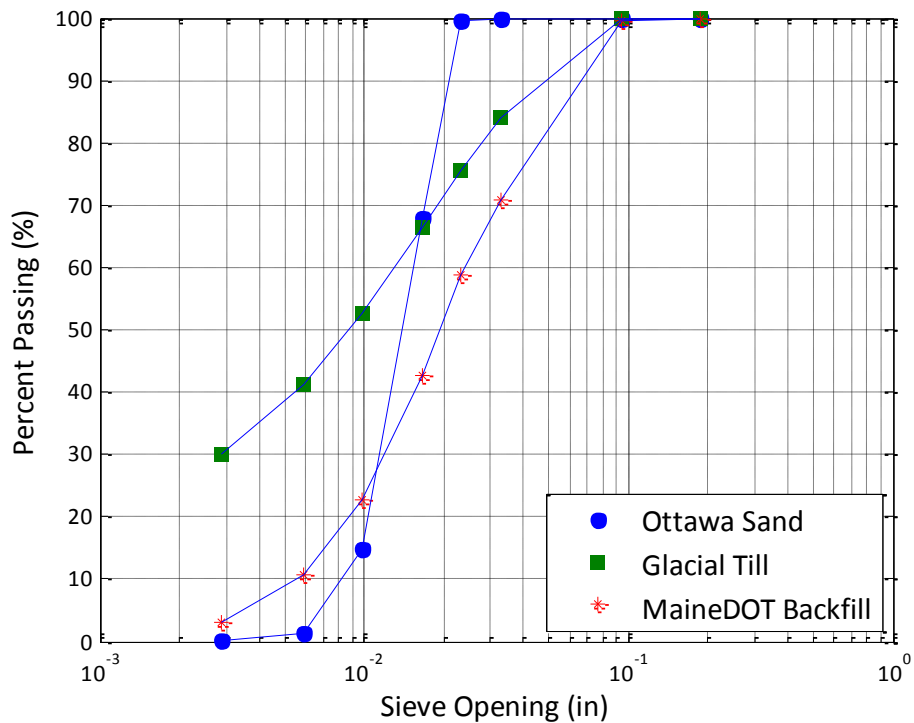


Figure 16: Grain Size Distribution Results

10.2. Specific Gravity

Specific gravity tests were done in accordance with ASTM D854. The reported specific gravities are the average of 3 tests. Specific gravity testing can be seen in Figure 17.



Figure 17: Specific Gravity Test

Specific gravity measurements have been corrected to 20 degrees Centigrade. A specific gravity of 2.65 was used for Ottawa Sand. The results of specific gravity testing can be seen below in Table 8.

Table 8: Specific Gravity Results

Soil	Trial 1	Trial 2	Trial 3	Average
MDOT Backfill	2.72	2.74	2.71	2.72
Glacial Till	2.70	2.71	2.70	2.70

10.3. Maximum and Minimum Density

Maximum density testing was conducted in accordance with ASTM D4253 Method 1A using a vibration frequency of 60 Hz. Minimum density testing was conducted in accordance with ASTM D4254 Method A.

During maximum density testing, some fine material escaped through the top of the mold. This is not believed to have a significant effect on the results for maximum density. The test fixture for maximum density testing can be seen in Figure 18.



Figure 18: Maximum Density Test

The glacial till had higher fines content than the other soils, which required the maximum density to be obtained through a modified proctor test. Modified proctor results can be seen in Figure 19.

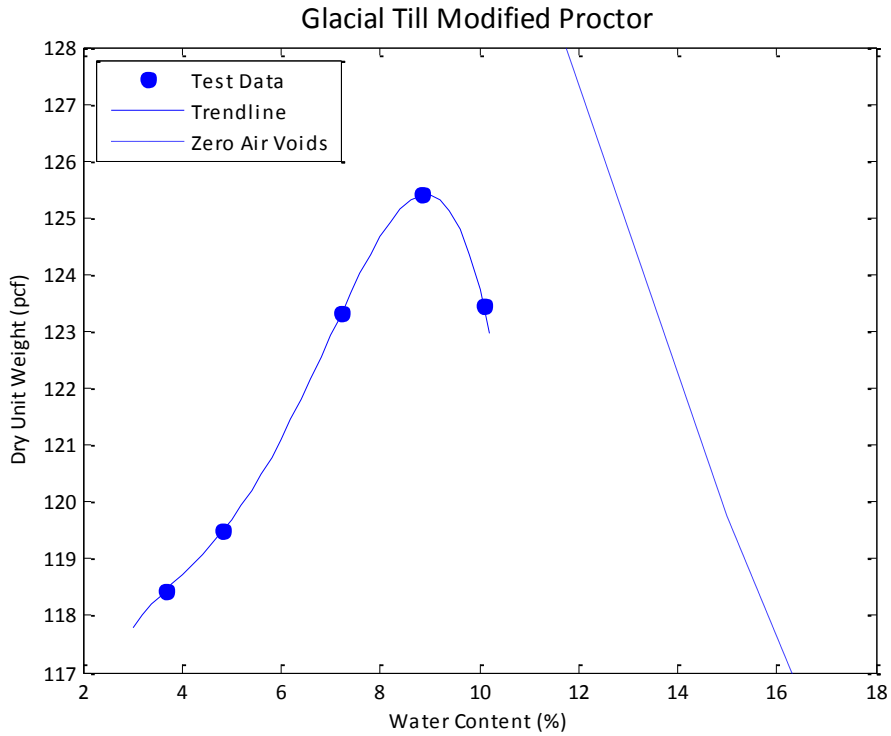


Figure 19: Modified Proctor Results for Glacial Till

A summary of the maximum and minimum density testing can be seen in Table 9.

Table 9: Maximum and Minimum Density Results

Soil	Minimum Density (pcf)	Maximum Density (pcf)	Minimum Void Ratio	Maximum Void Ratio
Ottawa Sand	96.8	114.1	0.45	0.71
MDOT Backfill	98.8	122.6	0.39	0.72
Glacial Till	85.0	125.5	0.34	0.98

10.4. Atterberg Limits

Atterberg limits were found for the glacial till due to its high fines content. This testing was conducted in accordance with ASTM D4318.

The results of the liquid limit test can be seen in Figure 20.

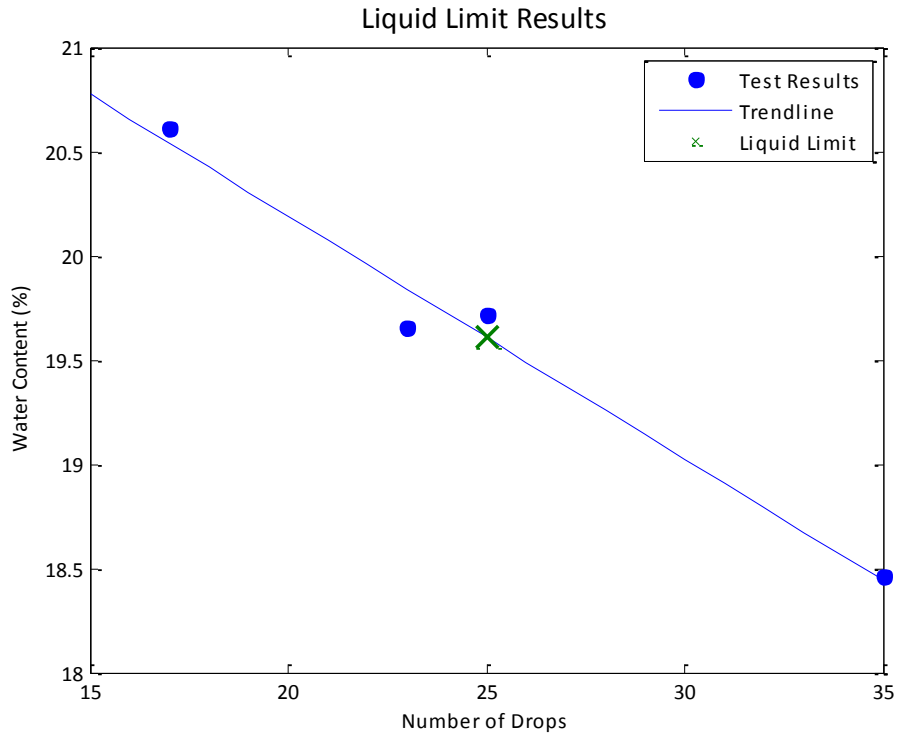


Figure 20: Liquid Limit Results

A summary of the Atterberg limits for the glacial till can be seen in Table 10.

Table 10: Atterberg Limits Results for Glacial Till

Glacial Till Results	
Liquid Limit	19.6
Plastic Limit	16.8
Plasticity Index	2.8

10.5. Direct Shear (Soil-Soil)

Direct shear testing was conducted in accordance with ASTM D3080. Each soil was tested at a target relative density of 50-55% and 70-75% prior to consolidation using pressures of 1000, 2000, and 5000 psf. The test frame can be seen in Figure 21.



Figure 21: Direct Shear Test

Results of direct shear testing can be seen in Table 11.

Table 11: Direct Shear Results

Soil	Density	Peak (Degrees)	Constant Volume (Degrees)
Ottawa Sand	Medium Dense	36.4	31.5
	Dense	39.1	34.5
MDOT Backfill	Medium Dense	40.9	39.1
	Dense	42.1	35.3
Glacial Till	Medium Dense	39.4	38.4
	Dense	40.7	38.7

Results of individual direct shear tests can be seen in Appendix E.

10.6. Interface Friction (Soil-FRP)

Interface friction tests were conducted by removing the bottom half of the direct shear box and replacing it with an FRP plate. The difference between direct shear and interface friction test fixtures can be seen in Figure 22.

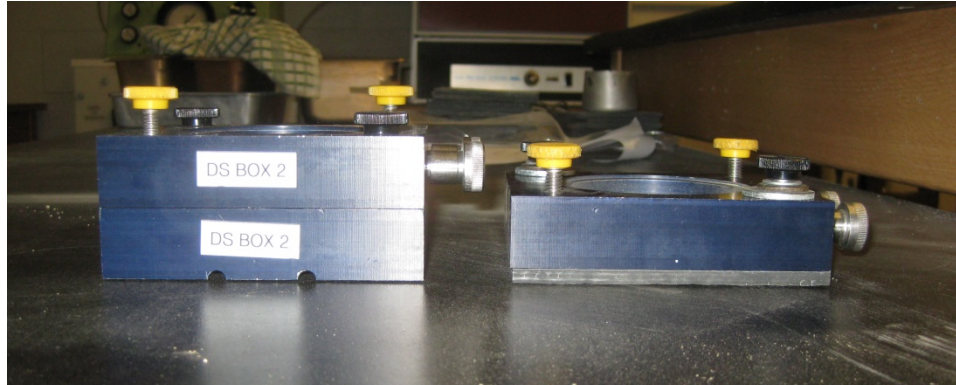


Figure 22: Direct Shear (Left) and Interface Friction (Right) Test Fixtures

Interface friction tests were also conducted at target relative densities of 50-55% and 70-75% prior to consolidation using pressures of 1000, 2000, and 5000 psf. FRP plates were not perfectly flat, which allowed soil grains to escape during compaction and consolidation. This led to errors in relative density calculations. A constant compactive effort was used to prepare samples as closely as possible to the relative densities used in direct shear tests. Results of the interface friction tests can be seen in Table 12.

Table 12: Interface Friction Results

Soil	Density	Peak (Degrees)	Constant Volume (Degrees)
Ottawa Sand	Medium Dense	28.2	26.3
	Dense	32.6	27.3
MDOT Backfill	Medium Dense	28.4	28.2
	Dense	31.8	28.9
Glacial Till	Medium Dense	31.6	30.9
	Dense	32.3	32.1

Results of individual interface friction tests can be seen in Appendix F.

11. Discussion

Results of the coupon level tests show that the FRP composite plates can be modeled as an orthotropic material.

The error in strain measurement is approximately +/- 500 microstrain because the camera system used in ARAMIS is sensitive to small vibrations. Vibrations can be caused by the

hydraulic system used in the laboratory, temperature and humidity control systems, and nearby activity in the laboratory. This error is relatively small when measuring strains in the direction of loading, but it will be larger when measuring strains perpendicular to the direction of loading because the ultimate strain is smaller. This can lead to error in calculating Poisson's ratio. Poisson's ratio calculations using longitudinal tension coupons are considered the most representative because the area for strain measurement is the largest. This allows some of the error in the measurement to be averaged out. Poisson's ratio (ν_{xy}) was found to be 0.31 with a coefficient of variation of 13.6%.

12. Conclusions

A summary of coupon level mechanical properties can be seen in Table 13.

Table 13: Average Mechanical Properties of FRP Plates

Test	Orientation of Properties	Ultimate Strength (ksi)	Ultimate Strain (Microstrain)	Modulus (ksi)	Poisson's Ratio
Longitudinal Tension	X	76.9	2.56E+04	3.26E+03	0.31 (ν_{xy})
Hoop Tension	Y	25.3	2.27E+04	1.98E+03	–
Longitudinal Compression	X	72.0	-2.17E+04	3.67E+03	–
Hoop Compression	Y	34.7	-1.65E+04	2.14E+03	–
In-Plane Shear	XY	22.3	2.88E+04	8.49E+02	–

Stress-strain relationships of representative tension and compression samples are presented in Figure 23.

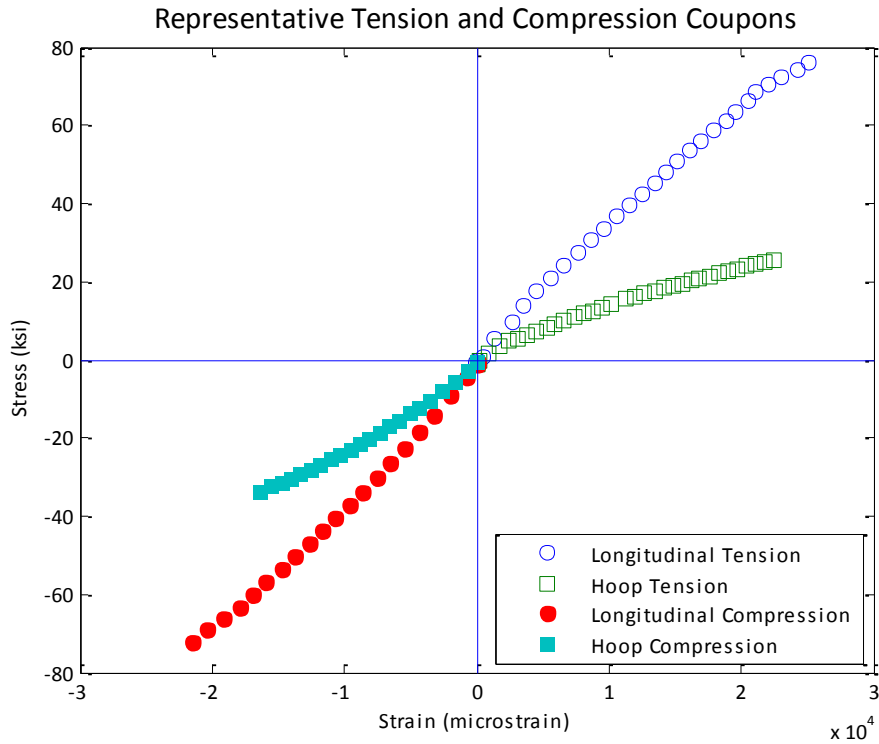


Figure 23: Representative Tension and Compression Samples

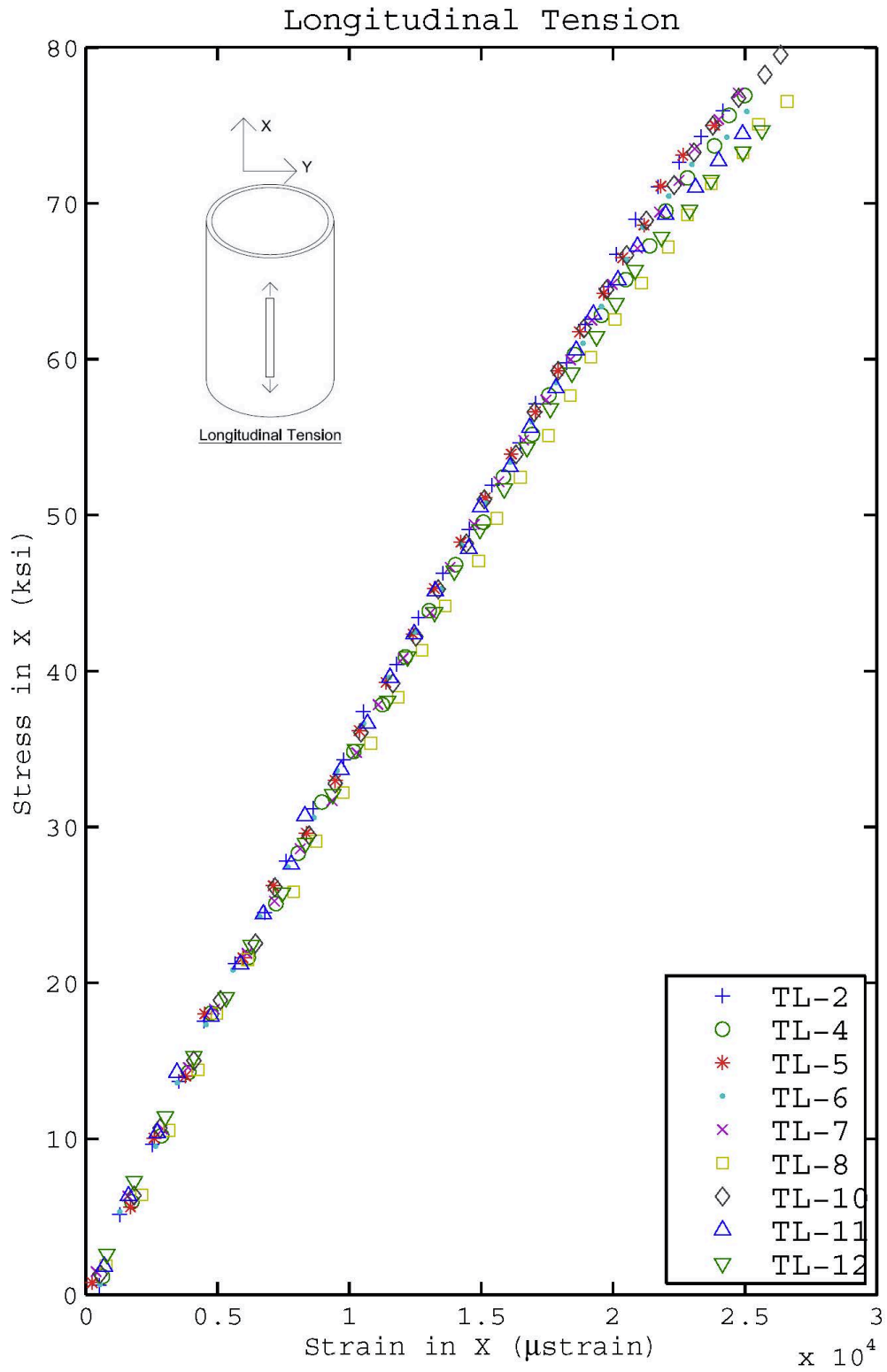
A summary of soil friction test results can be seen in Table 14.

Table 14: Summary of Soil Friction Testing

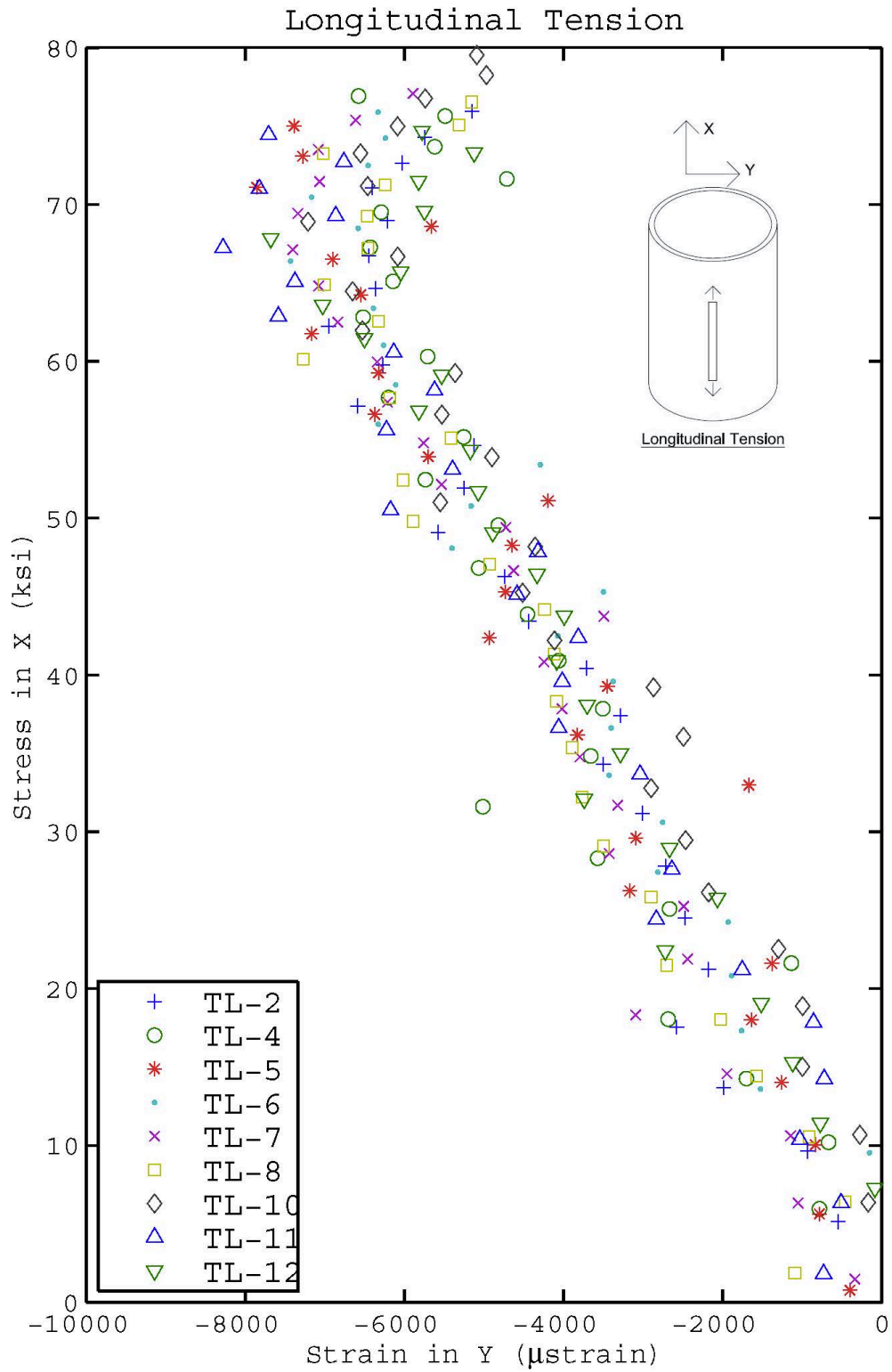
Sample		Direct Shear		Interface Friction	
Soil	Density	Peak (Degrees)	Constant Volume (Degrees)	Peak (Degrees)	Constant Volume (Degrees)
Ottawa Sand	Medium Dense	36.4	31.5	28.2	26.3
	Dense	39.1	34.5	32.6	27.3
MDOT Backfill	Medium Dense	40.9	39.1	28.4	28.2
	Dense	42.1	35.3	31.8	28.9
Glacial Till	Medium Dense	39.4	38.4	31.6	30.9
	Dense	40.7	38.7	32.3	32.1

Appendix A: Tension Results

Tension Results



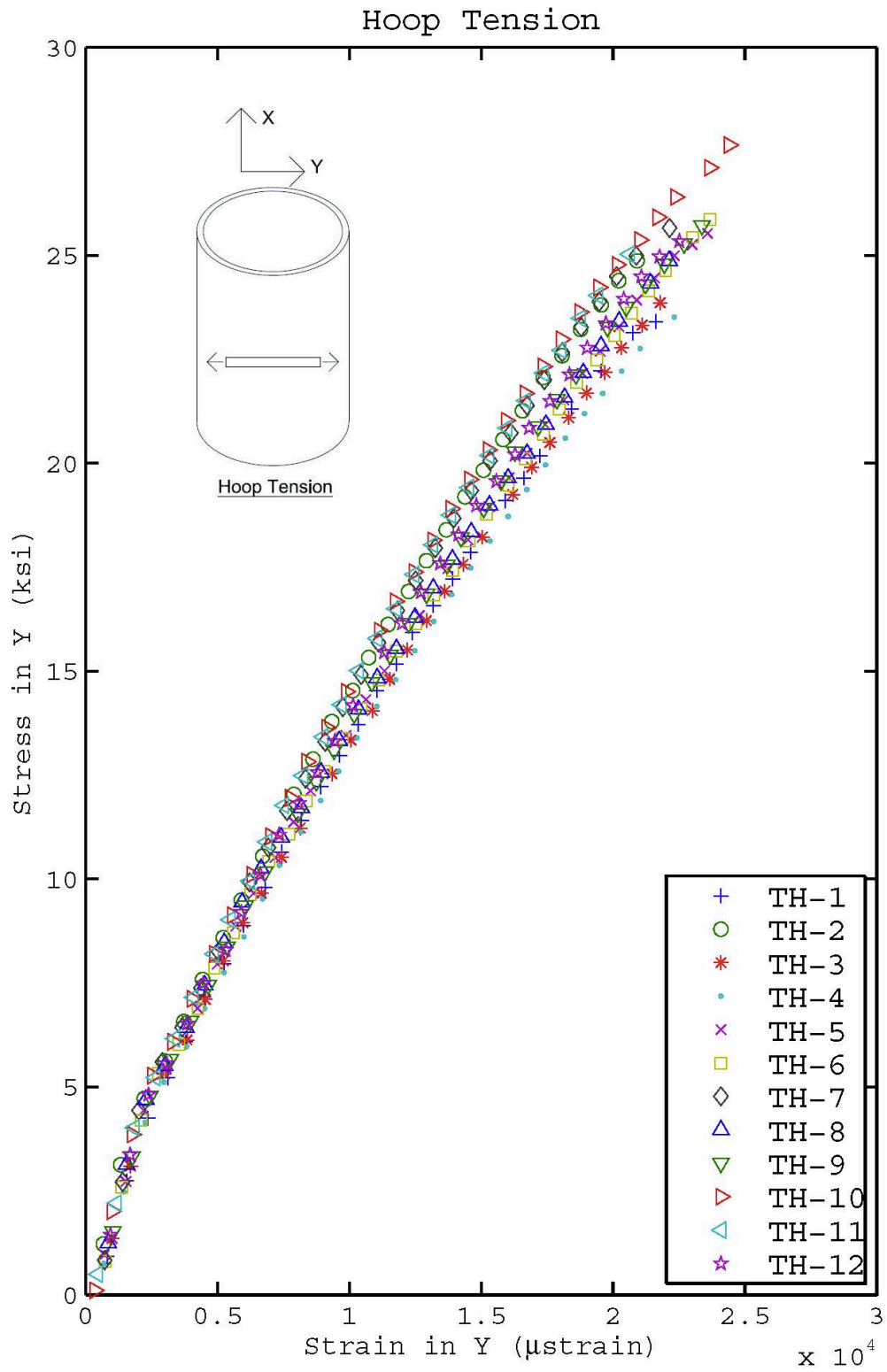
Tension Results



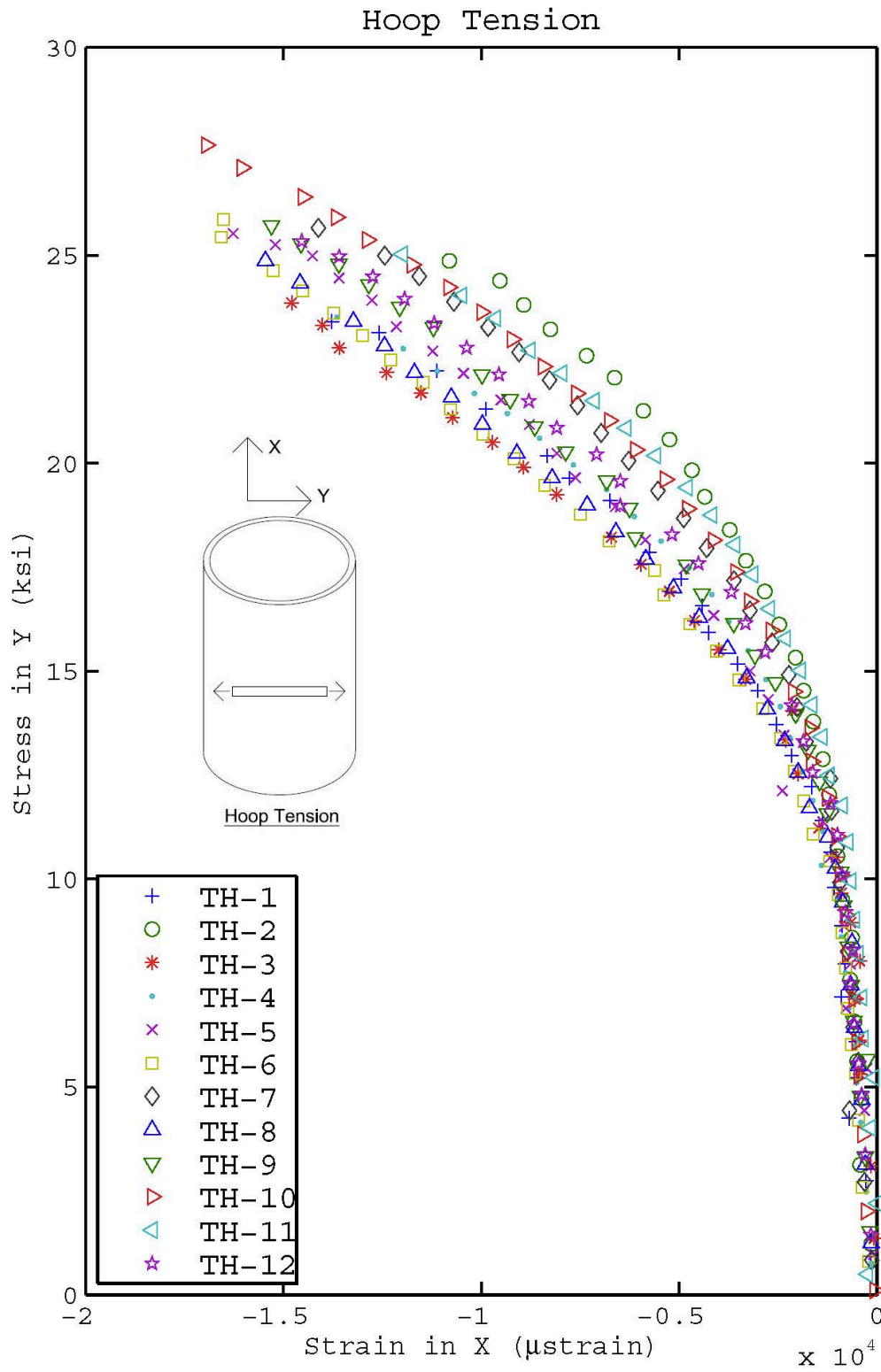
Tension Results

Longitudinal Tension Test Results							
Sample	Ultimate Stress (ksi)	Ultimate Strain in X (microstrain)	Ultimate Strain in Y (microstrain)	Modulus of Elasticity (Linear Regression) (ksi)	Modulus of Elasticity (Chord) (ksi)	Poisson Ratio (Linear Regression)	Poisson Ratio (Chord)
TL-2	77.1	2.48E+04	-5.68E+03	3.33E+03	3.37E+03	0.23	0.36
TL-4	77.3	2.54E+04	-5.45E+03	3.12E+03	2.86E+03	0.33	0.31
TL-5	75.3	2.38E+04	-7.06E+03	3.32E+03	3.43E+03	0.28	0.28
TL-6	76.9	2.57E+04	-5.27E+03	3.27E+03	3.24E+03	0.32	0.38
TL-7	78.3	2.57E+04	-6.26E+03	3.33E+03	3.45E+03	0.36	0.42
TL-8	77.1	2.68E+04	-4.80E+03	3.20E+03	3.27E+03	0.33	0.28
TL-10	79.9	2.66E+04	-5.29E+03	3.35E+03	3.44E+03	0.37	0.60
TL-11	74.4	2.49E+04	-7.71E+03	3.25E+03	3.23E+03	0.29	0.34
TL-12	75.6	2.66E+04	-5.31E+03	3.20E+03	3.21E+03	0.32	0.36
Mean	76.9	2.56E+04	-5.87E+03	3.26E+03	3.28E+03	0.31	0.37
Std. Dev.	1.6	9.85E+02	9.56E+02	7.73E+01	1.83E+02	0.04	0.10
COV	2.14%	3.85%	16.28%	2.37%	5.59%	13.55%	26.68%

Tension Results



Tension Results

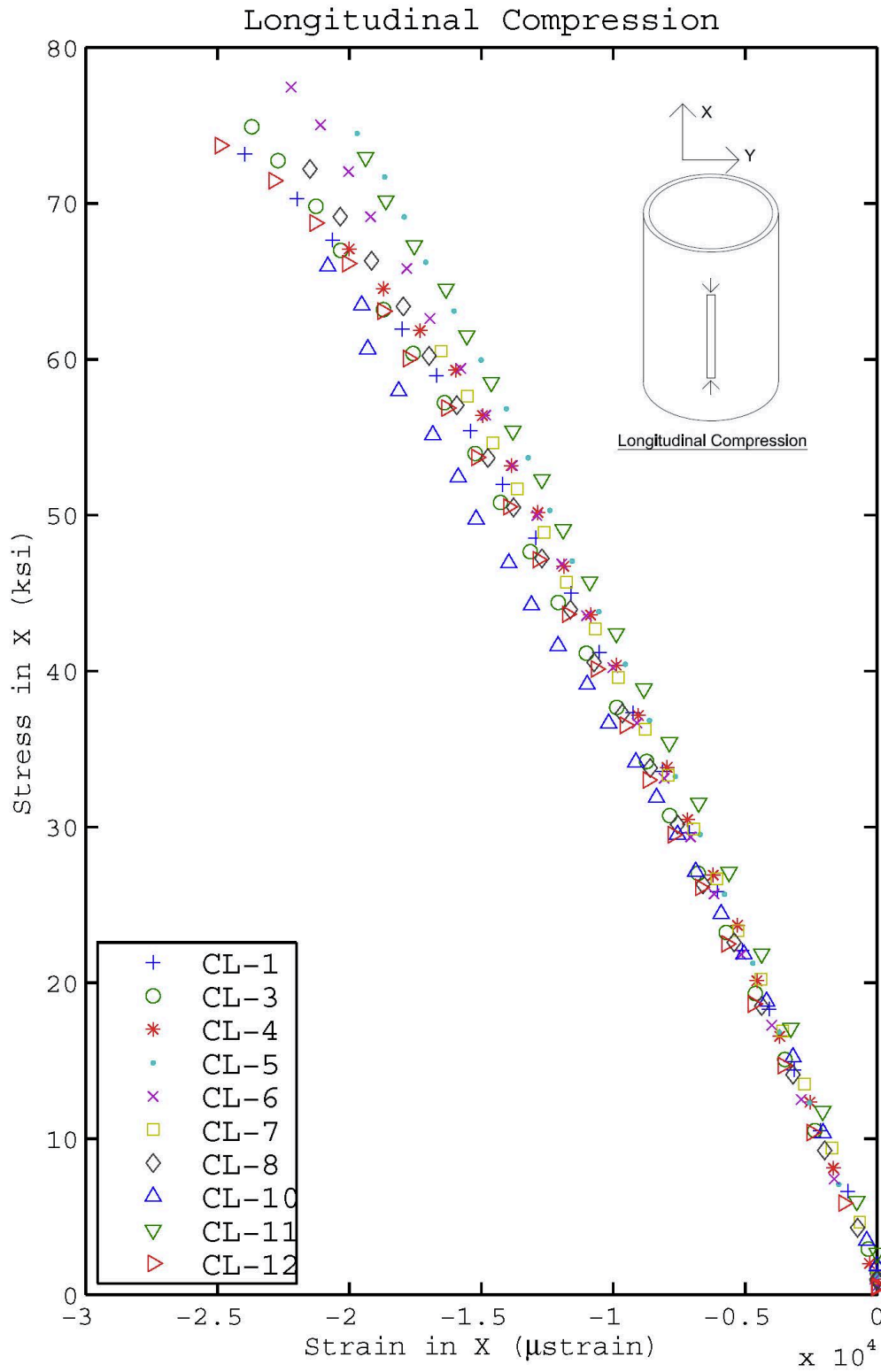


Tension Results

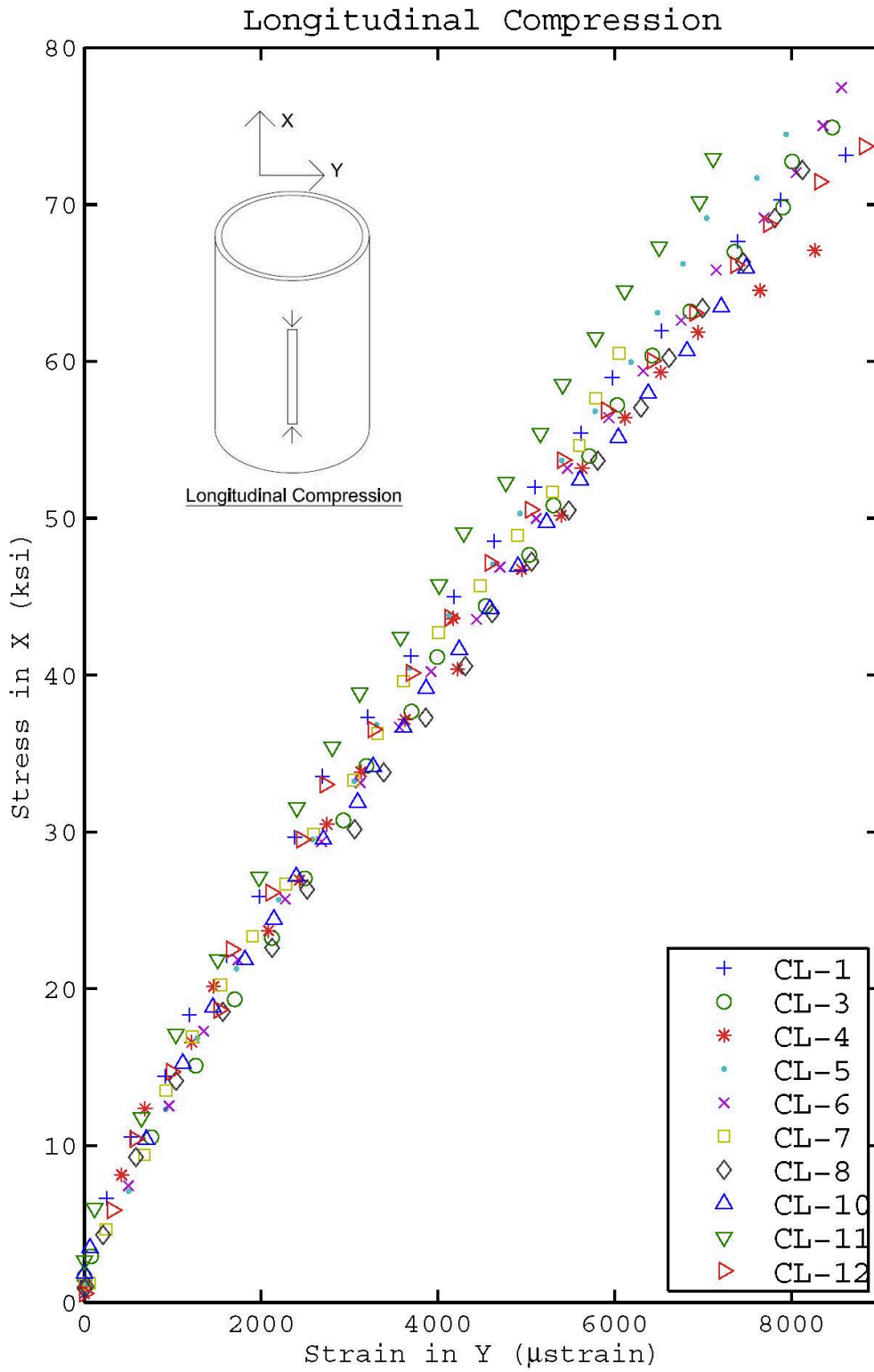
Hoop Tension Test Results							
Sample	Ultimate Stress (ksi)	Ultimate Strain in Y (microstrain)	Ultimate Strain in X (microstrain)	Modulus of Elasticity (Linear Regression) (ksi)	Modulus of Elasticity (Chord) (ksi)	Poisson Ratio (Linear Regression)	Poisson Ratio (Chord)
TH-1	23.5	2.20E+04	-1.43E+04	1.93E+03	1.88E+03	0.15	0.12
TH-2	25.0	2.12E+04	-1.12E+04	1.76E+03	1.79E+03	0.11	0.14
TH-3	23.9	2.19E+04	-1.50E+04	2.07E+03	2.00E+03	0.18	0.18
TH-4	23.9	2.27E+04	-1.43E+04	1.86E+03	1.84E+03	0.26	0.20
TH-5	25.5	2.36E+04	-1.63E+04	1.91E+03	1.84E+03	0.16	0.06
TH-6	26.1	2.41E+04	-1.74E+04	2.05E+03	1.99E+03	0.14	0.15
TH-7	25.8	2.24E+04	-1.45E+04	2.02E+03	1.98E+03	0.17	0.17
TH-8	25.1	2.26E+04	-1.59E+04	2.02E+03	1.93E+03	0.16	0.15
TH-9	26.0	2.40E+04	-1.60E+04	2.10E+03	1.99E+03	0.18	0.15
TH-10	27.6	2.44E+04	-1.69E+04	1.91E+03	1.85E+03	0.16	0.10
TH-11	25.4	2.10E+04	-1.24E+04	2.05E+03	2.03E+03	0.14	0.18
TH-12	25.4	2.26E+04	-1.48E+04	2.08E+03	2.02E+03	0.19	0.13
Mean	25.3	2.27E+04	-1.49E+04	1.98E+03	1.93E+03	0.17	0.14
Std. Dev.	1.1	1.10E+03	1.78E+03	1.03E+02	8.42E+01	0.04	0.04
COV	4.52%	4.86%	11.97%	5.19%	4.36%	21.49%	26.19%

Appendix B: Compression Results

Compression Results



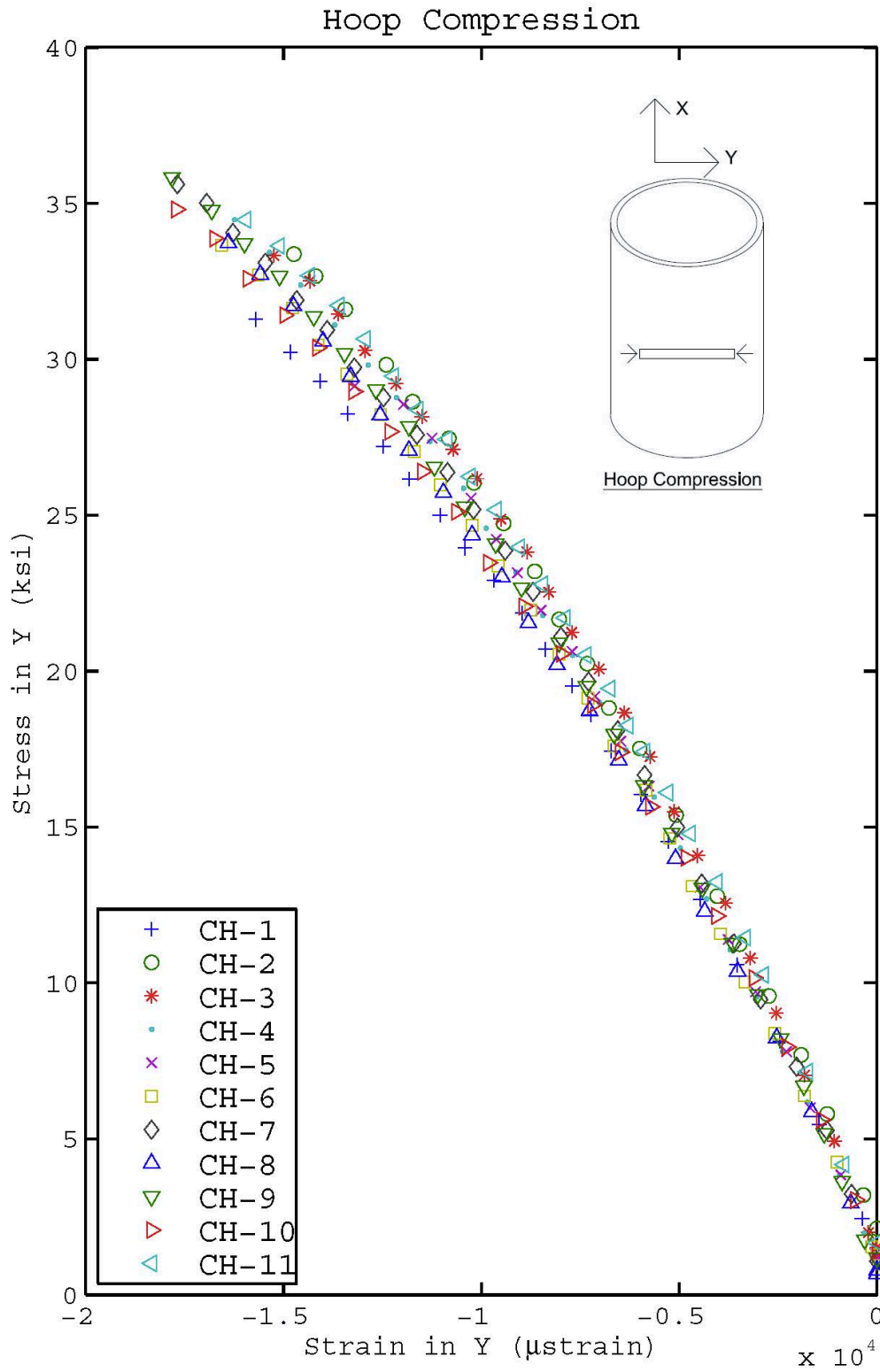
Compression Results



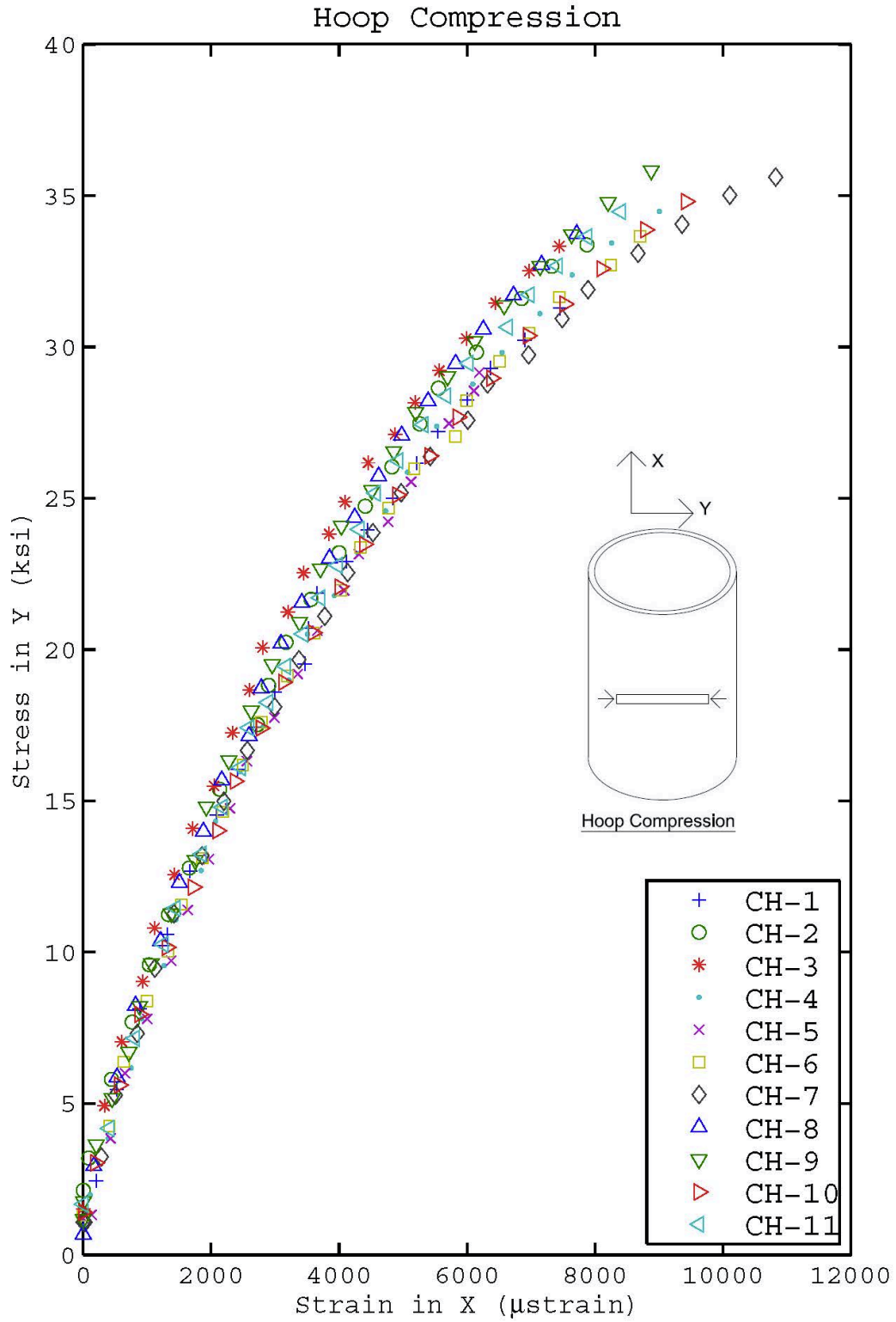
Compression Results

Longitudinal Compression Test Results							
Sample	Ultimate Stress (ksi)	Ultimate Strain in X (microstrain)	Ultimate Strain in Y (microstrain)	Modulus of Elasticity (Linear Regression) (ksi)	Modulus of Elasticity (Chord) (ksi)	Poisson Ratio (Linear Regression)	Poisson Ratio (Chord)
CL-1	75.7	-2.56E+04	9.16E+03	-3.72E+03	-3.70E+03	0.38	0.38
CL-3	76.3	-2.50E+04	8.61E+03	-3.57E+03	-3.57E+03	0.38	0.37
CL-4	67.6	-2.03E+04	8.45E+03	-3.78E+03	-3.86E+03	0.43	0.46
CL-5	74.5	-1.97E+04	7.94E+03	-4.02E+03	-3.98E+03	0.41	0.40
CL-6	78.0	-2.27E+04	8.78E+03	-3.83E+03	-3.84E+03	0.43	0.42
CL-7	62.1	-1.71E+04	6.15E+03	-3.67E+03	-3.65E+03	0.39	0.38
CL-8	72.6	-2.18E+04	8.02E+03	-3.57E+03	-3.54E+03	0.43	0.43
CL-10	66.5	-2.03E+04	7.56E+03	-3.09E+03	-3.10E+03	0.36	0.33
CL-11	72.9	-1.94E+04	7.12E+03	-3.82E+03	-3.86E+03	0.38	0.38
CL-12	74.1	-2.55E+04	8.99E+03	-3.62E+03	-3.68E+03	0.37	0.40
Mean	72.0	-2.17E+04	8.08E+03	-3.67E+03	-3.68E+03	0.40	0.39
Std. Dev.	5.0	2.90E+03	9.33E+02	2.46E+02	2.48E+02	0.03	0.04
COV	6.99%	13.36%	11.55%	6.70%	6.73%	6.73%	9.14%

Compression Results



Compression Results

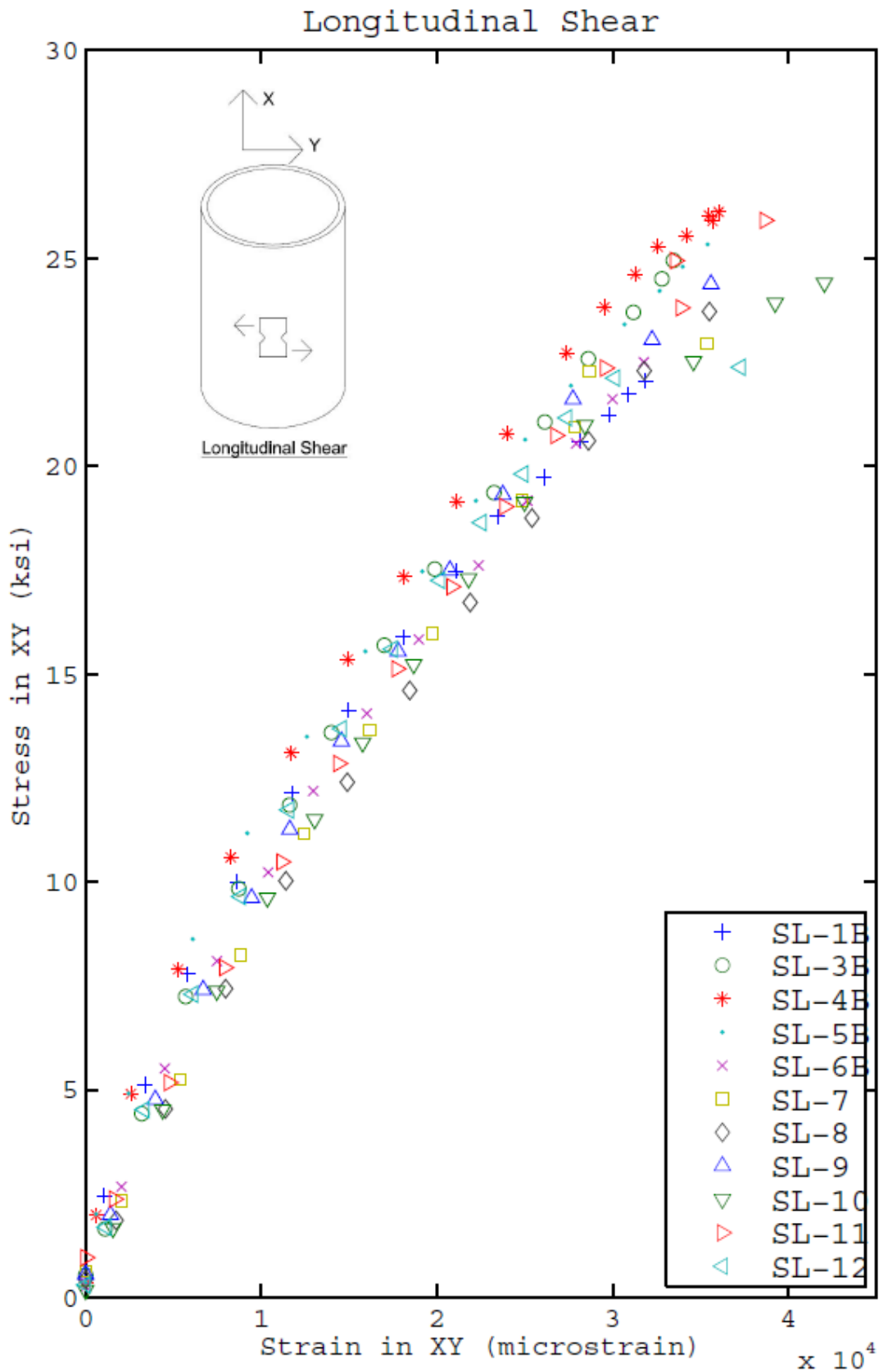


Compression Results

Hoop Compression Test Results							
Sample	Ultimate Stress (ksi)	Ultimate Strain in Y (microstrain)	Ultimate Strain in X (microstrain)	Modulus of Elasticity (Linear Regression) (ksi)	Modulus of Elasticity (Chord) (ksi)	Poisson Ratio (Linear Regression)	Poisson Ratio (Chord)
CH-1	31.9	-1.62E+04	7.84E+03	-1.99E+03	-1.95E+03	0.45	0.44
CH-2	34.0	-1.50E+04	8.12E+03	-2.22E+03	-2.19E+03	0.51	0.52
CH-3	33.3	-1.52E+04	7.44E+03	-2.20E+03	-2.22E+03	0.48	0.48
CH-4	35.2	-1.68E+04	9.51E+03	-2.21E+03	-2.22E+03	0.51	0.52
CH-5	29.9	-1.38E+04	6.50E+03	-2.19E+03	-2.24E+03	0.52	0.54
CH-6	33.9	-1.67E+04	8.81E+03	-2.12E+03	-2.08E+03	0.50	0.50
CH-7	35.7	-1.79E+04	1.11E+04	-2.15E+03	-2.14E+03	0.52	0.52
CH-8	34.3	-1.68E+04	7.94E+03	-2.11E+03	-2.14E+03	0.44	0.45
CH-9	36.5	-1.84E+04	9.28E+03	-2.14E+03	-2.14E+03	0.45	0.46
CH-10	35.6	-1.89E+04	9.64E+03	-2.04E+03	-2.08E+03	0.48	0.49
CH-11	34.7	-1.61E+04	8.67E+03	-2.17E+03	-2.23E+03	0.49	0.51
Mean	34.1	-1.65E+04	8.62E+03	-2.14E+03	-2.15E+03	0.49	0.49
Std. Dev.	1.9	1.51E+03	1.25E+03	7.25E+01	8.71E+01	0.03	0.03
COV	5.57%	9.12%	14.51%	3.39%	4.05%	5.82%	6.31%

Appendix C: Shear Results

Shear Results

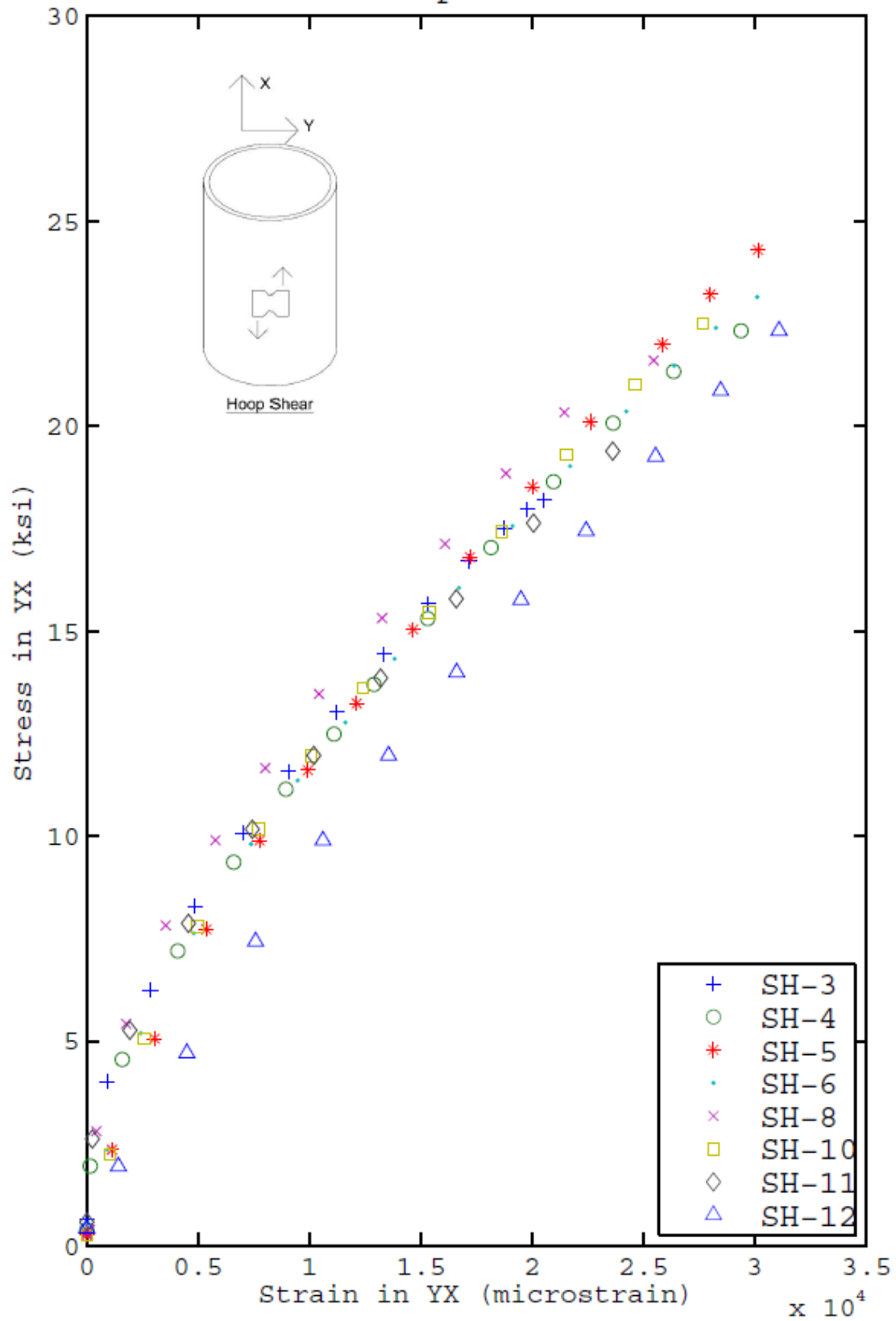


Shear Results

Longitudinal Shear Results				
Sample	Ultimate Stress (ksi)	Ultimate Strain XY (microstrain)	Shear Modulus (Linear Regression) (ksi)	Shear Modulus (Chord) (ksi)
SL-1B	22.2	3.18E+04	8.91E+02	8.93E+02
SL-3B	25.2	3.42E+04	9.13E+02	9.16E+02
SL-4B	26.1	3.60E+04	9.02E+02	9.00E+02
SL-5B	25.4	3.56E+04	8.86E+02	8.92E+02
SL-6B	22.9	3.24E+04	9.01E+02	9.10E+02
SL-7	23.4	3.20E+04	8.70E+02	8.62E+02
SL-8	24.8	4.08E+04	8.47E+02	8.39E+02
SL-9	24.4	3.56E+04	9.00E+02	8.96E+02
SL-10	24.4	4.40E+04	8.98E+02	8.96E+02
SL-11	25.9	3.86E+04	8.88E+02	8.73E+02
SL-12	22.6	3.81E+04	9.36E+02	9.39E+02
Mean	24.3	3.63E+04	8.94E+02	8.92E+02
Std. Dev.	1.4	3.86E+03	2.28E+01	2.70E+01
COV	5.57%	10.63%	2.55%	3.02%

Shear Results

Hoop Shear



Shear Results

Hoop Shear Results				
Sample	Ultimate Stress (ksi)	Ultimate Strain YX (microstrain)	Shear Modulus (Linear Regression) (ksi)	Shear Modulus (Chord) (ksi)
SH-3	18.2	2.06E+04	8.22E+02	8.41E+02
SH-4	23.1	3.12E+04	8.13E+02	8.23E+02
SH-5	25.1	3.21E+04	9.40E+02	9.53E+02
SH-6	23.5	3.12E+04	8.42E+02	8.51E+02
SH-8	21.9	2.61E+04	8.58E+02	8.78E+02
SH-10	23.0	2.94E+04	8.75E+02	8.90E+02
SH-11	20.2	2.65E+04	7.79E+02	7.78E+02
SH-12	23.3	3.36E+04	8.62E+02	8.47E+02
Mean	22.3	2.88E+04	8.49E+02	8.58E+02
Std. Dev.	2.1	4.23E+03	4.80E+01	5.15E+01
COV	9.63%	14.68%	5.65%	6.00%

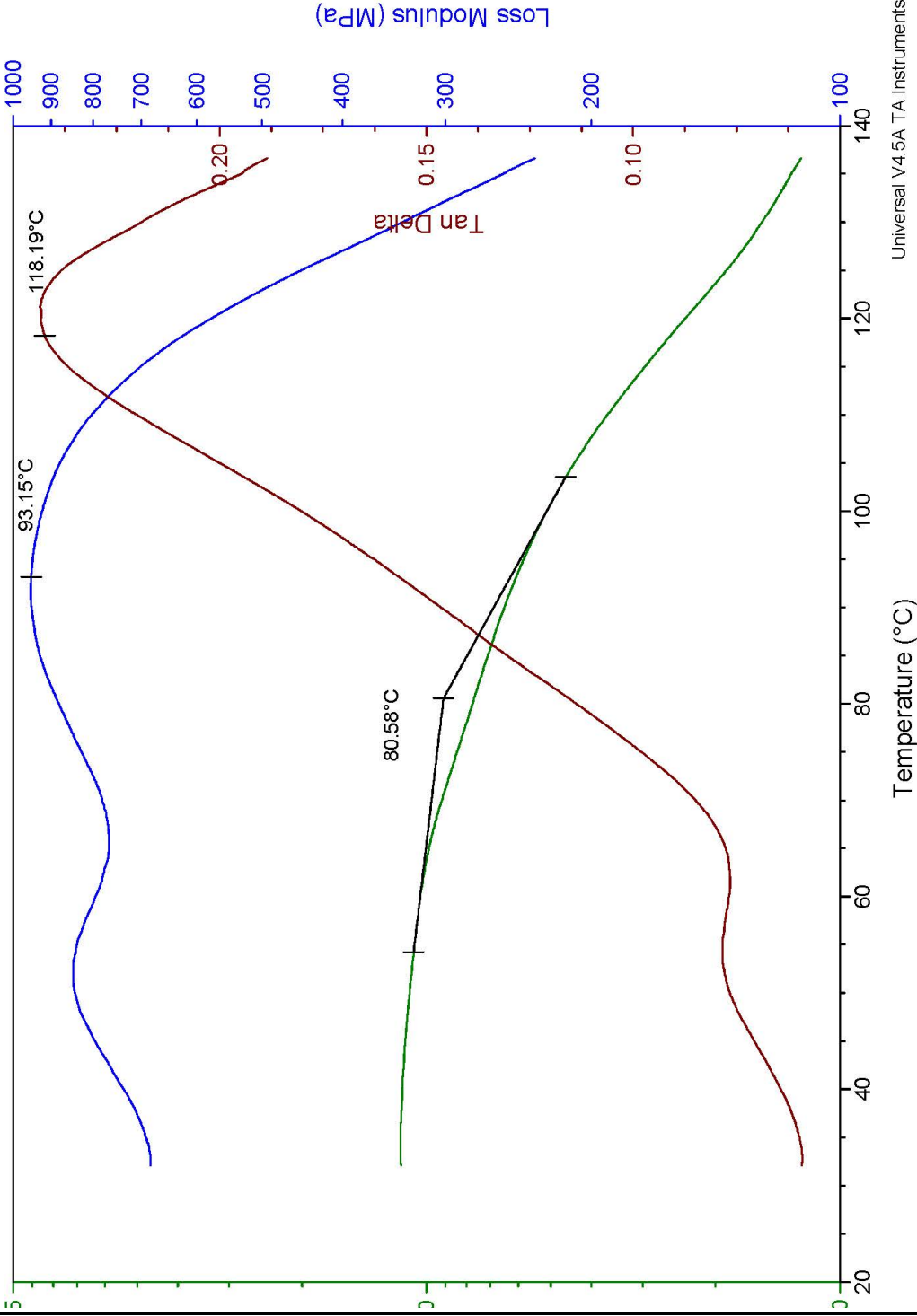
Appendix D: Glass Transition Temperature Results

Glass Transition Temperature Results

File: \\s5cfmxx\users\TA\Desktop\Date\Tg1_001
 Run Date: 15-Apr-2014 16:09
 Instrument: DMA Q800 V21.1 Build 51

DMA

Sample: Tg1
 Dimensions: 14.0233 x 5.2267 mm
 Test: Temperature Ramp
 Antenna: test



Universal V4.5A TA Instruments

UMaine Advanced Structures and Composites Center
 35 Flagstaff Rd
 University of Maine
 Orono, ME 04469

Telephone: 207-581-2123
 FAX: 207-581-2074
 composites@umit.maine.edu

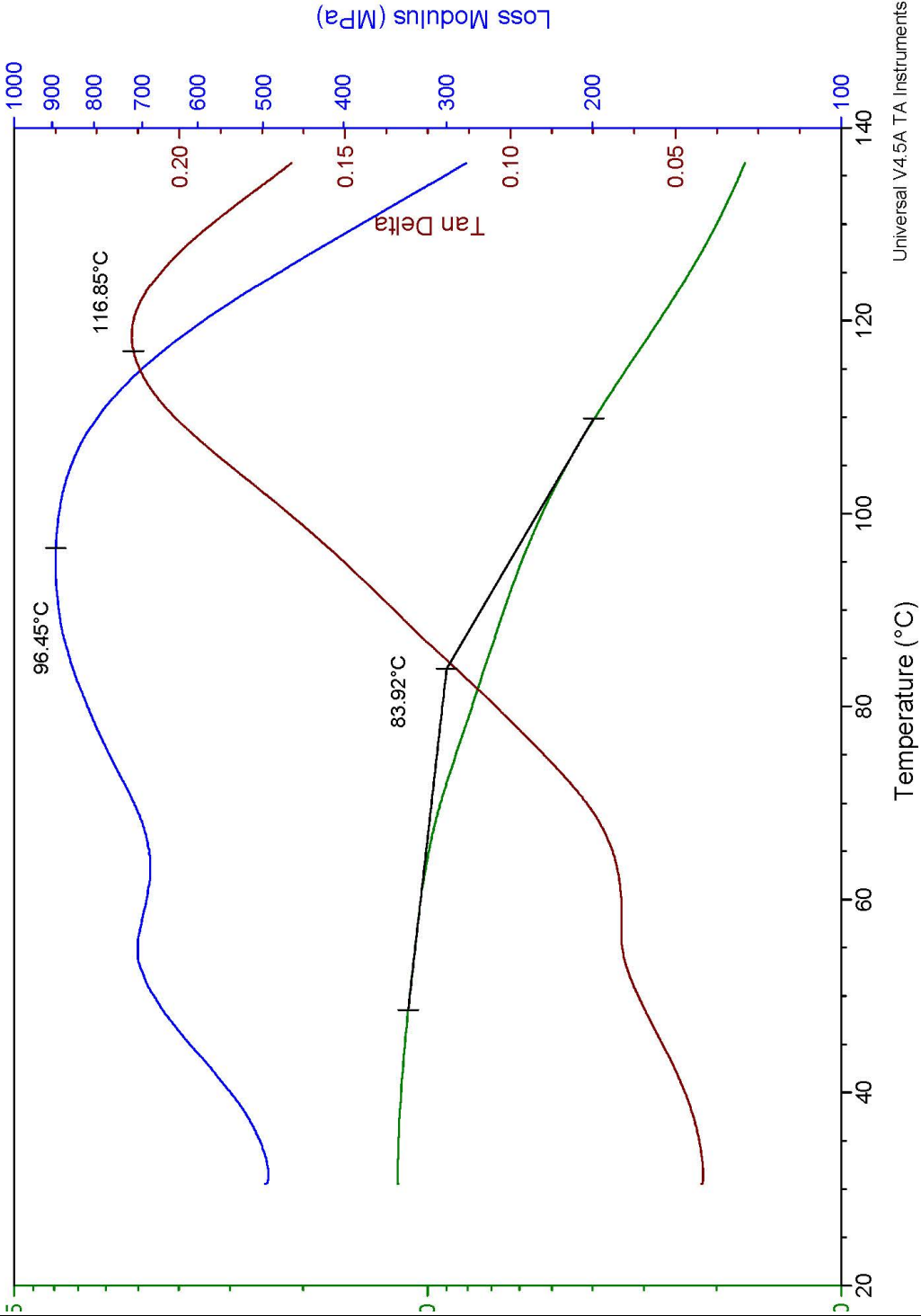
Glass Transition Temperature Results

File: \\s5cfmxxk\users\TA\Desktop\Date\Tg2.001

Run Date: 16-Apr-2014 07:58
Instrument: DMA Q800 V21.1 Build 51

DMA

Sample: Tg2
Dimensions: 10.0000 x 14.1900 x 4.9433 mm
Frequency: 1 Hz
Temperature Ramp
Antenna: test



Universal V4.5A TA Instruments

UMaine Advanced Structures and Composites Center
35 Flagstaff Rd
University of Maine
Orono, ME 04469

Telephone: 207-581-2123
FAX: 207-581-2074
composites@umit.maine.edu

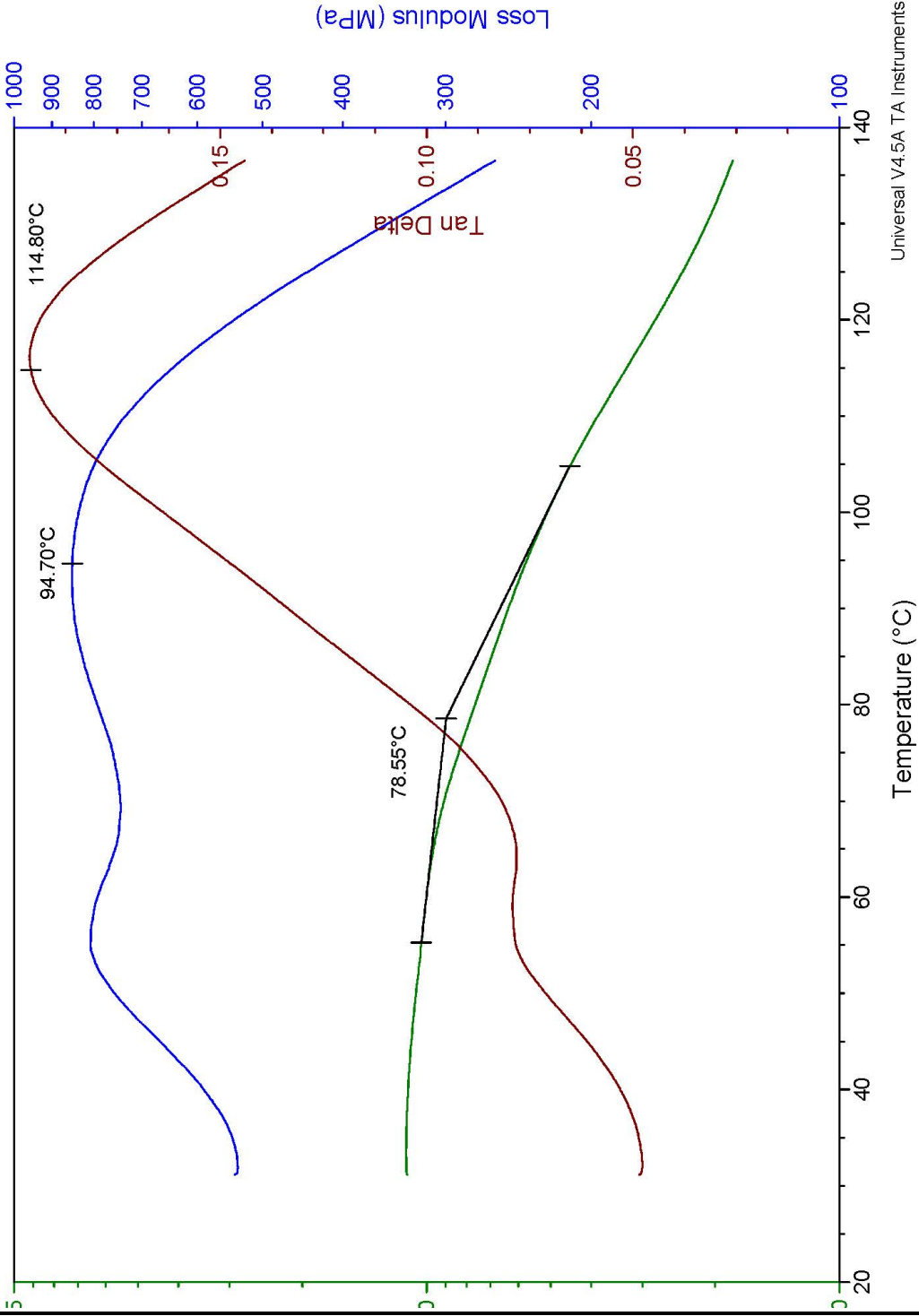
Glass Transition Temperature Results

File: \\s5cfmxx\users\TA\Desktop\Date\Tg3.001

Run Date: 16-Apr-2014 10:48
Instrument: DMA Q800 V21.1 Build 51

DMA

Sample: Tg3
Dimensions: 10.0000 x 14.0567 x 4.9967 mm
Test: Temperature Ramp
Ant: test



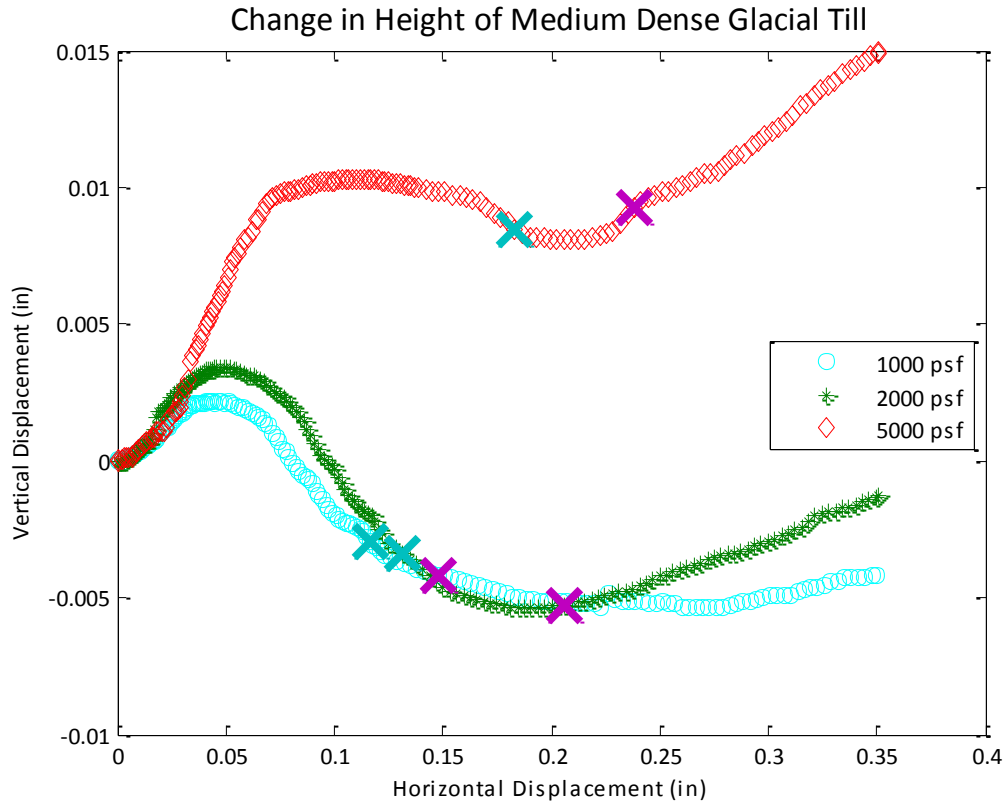
UMaine Advanced Structures and Composites Center
35 Flagstaff Rd
University of Maine
Orono, ME 04469

Telephone: 207-581-2123
FAX: 207-581-2074
composites@umit.maine.edu

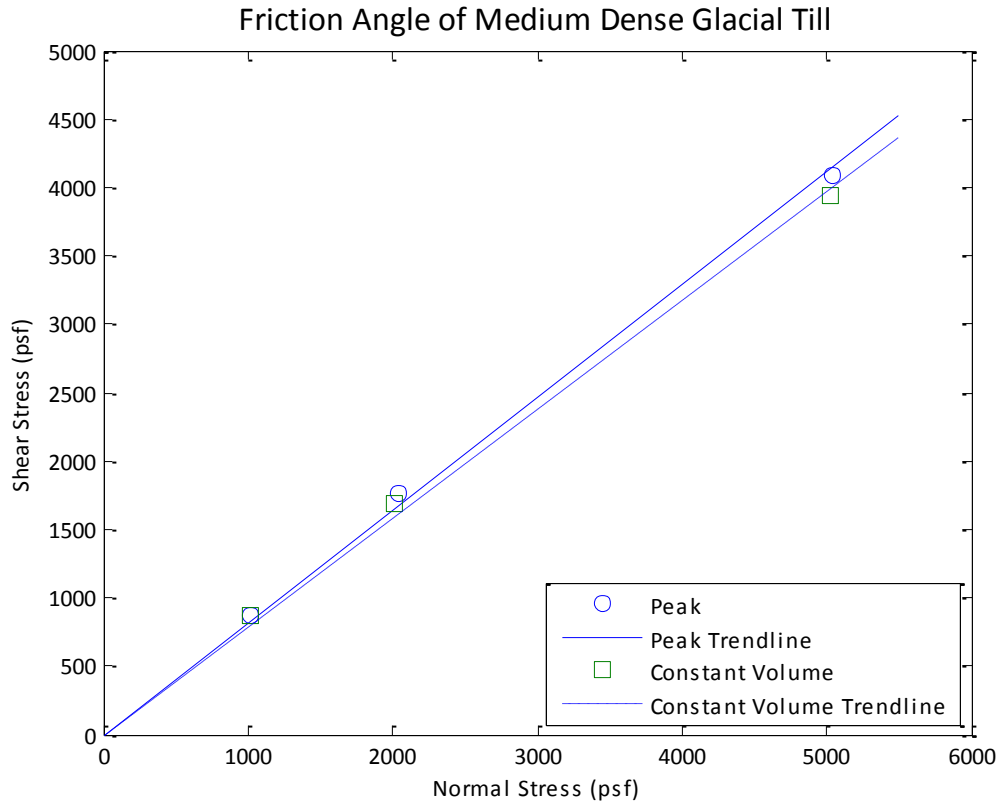
Glass Transition Temperature Results

Appendix E: Direct Shear Results

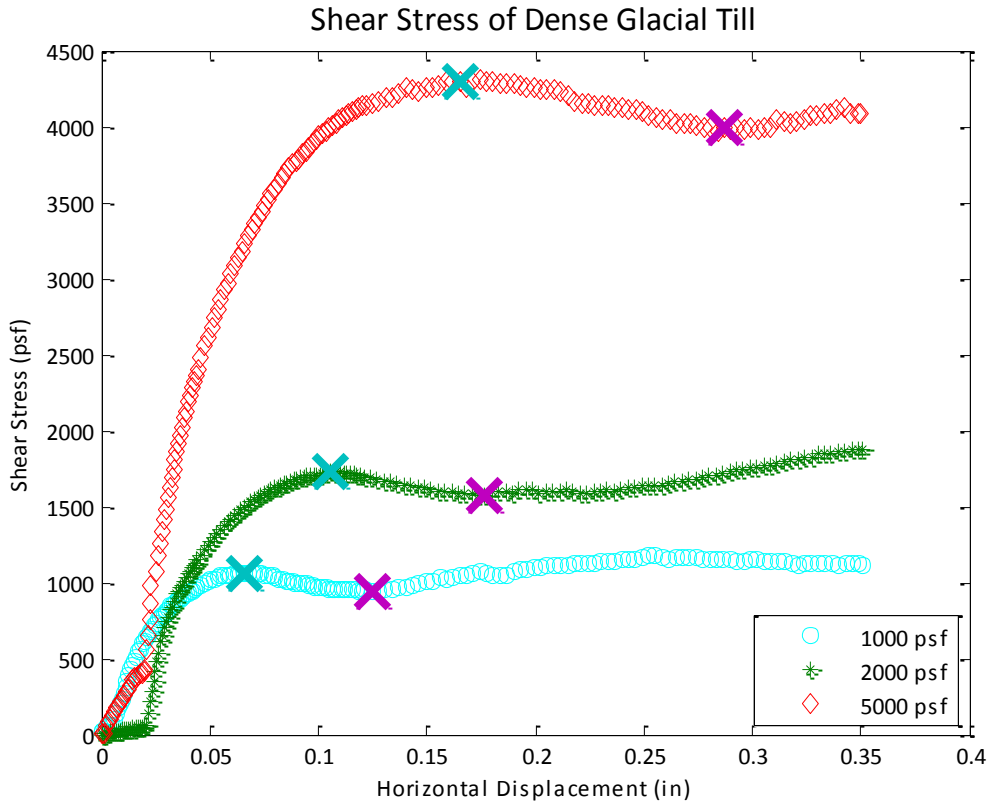
Direct Shear Results



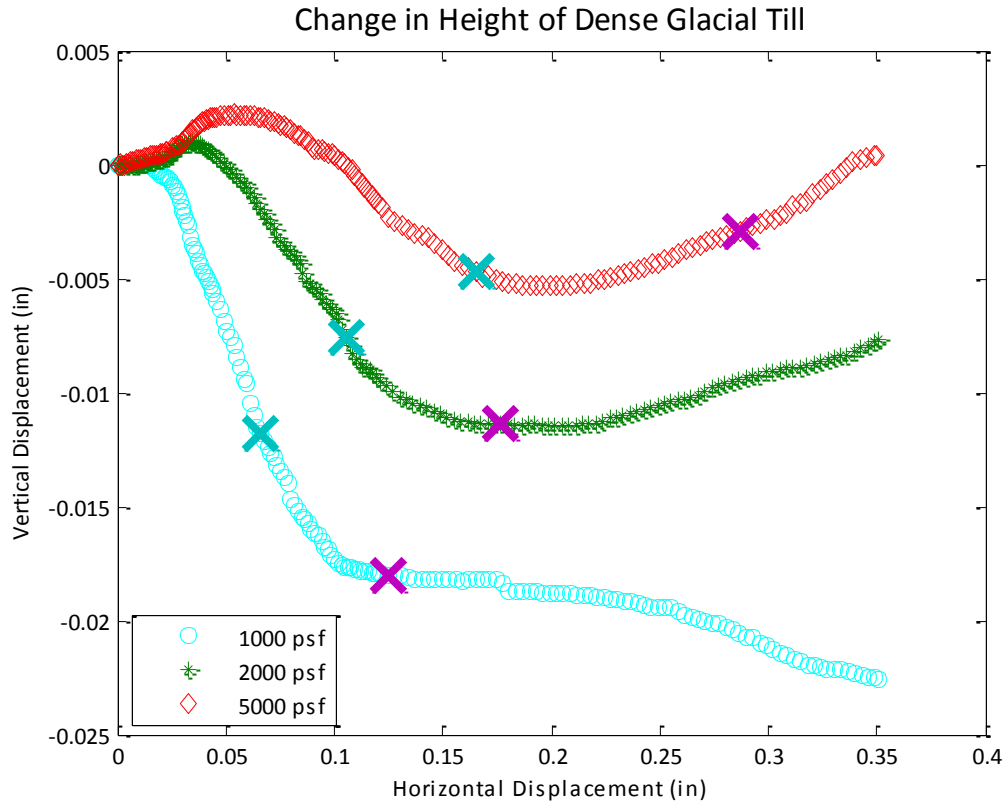
Direct Shear Results



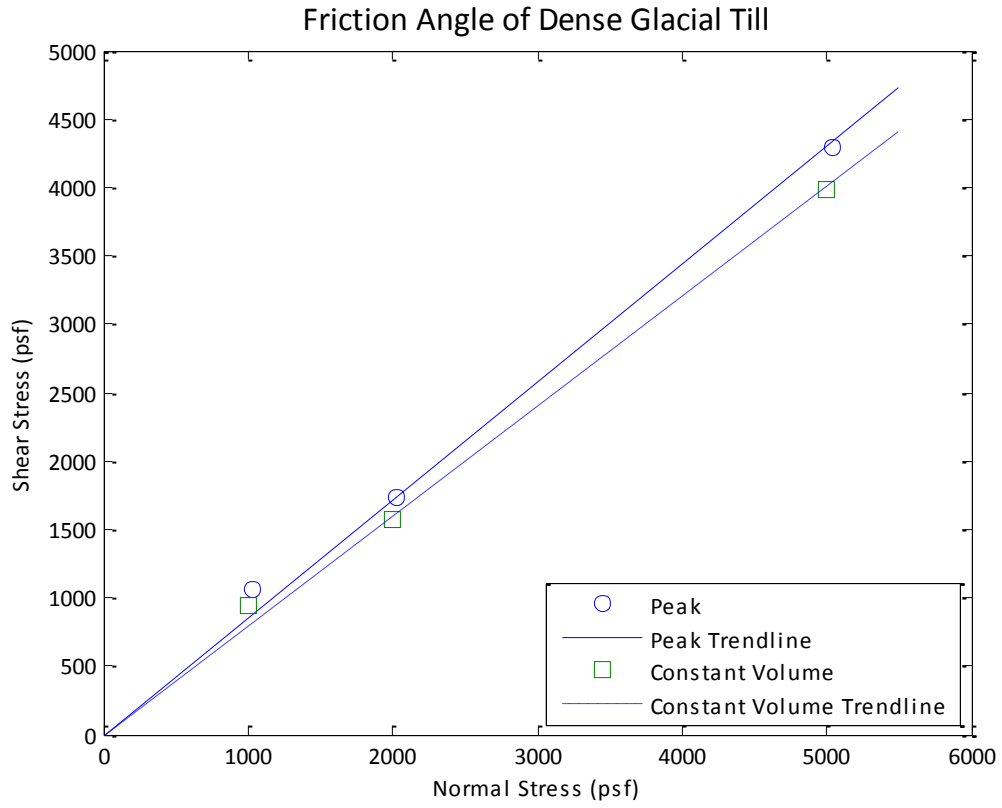
Direct Shear Results



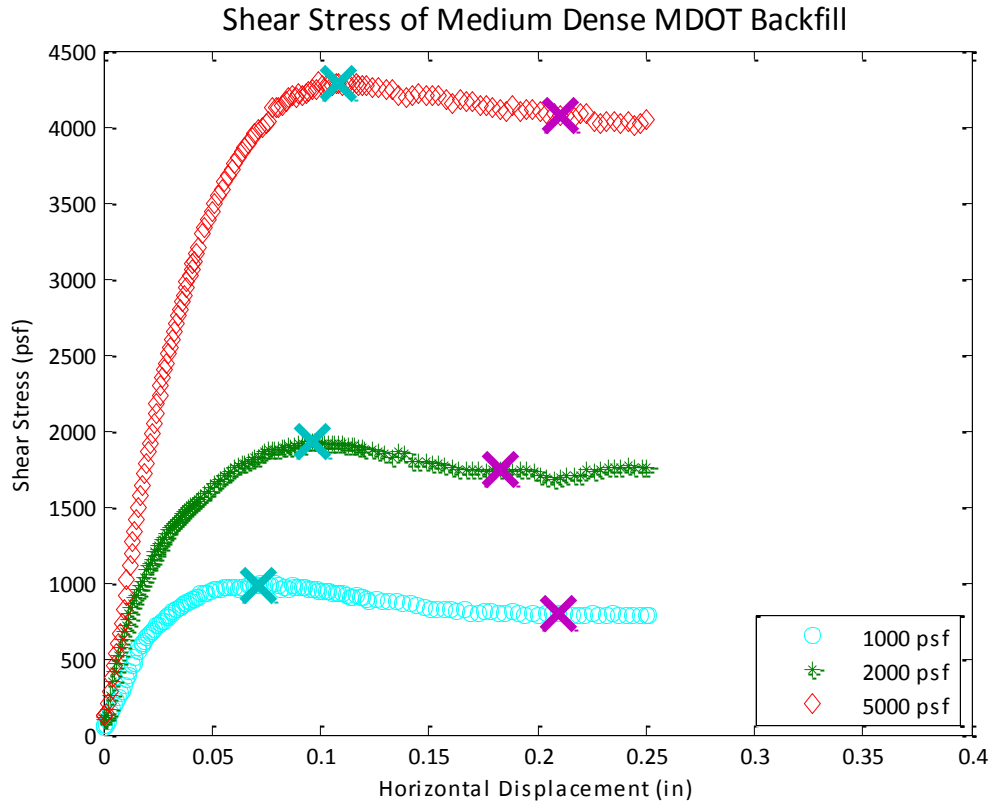
Direct Shear Results



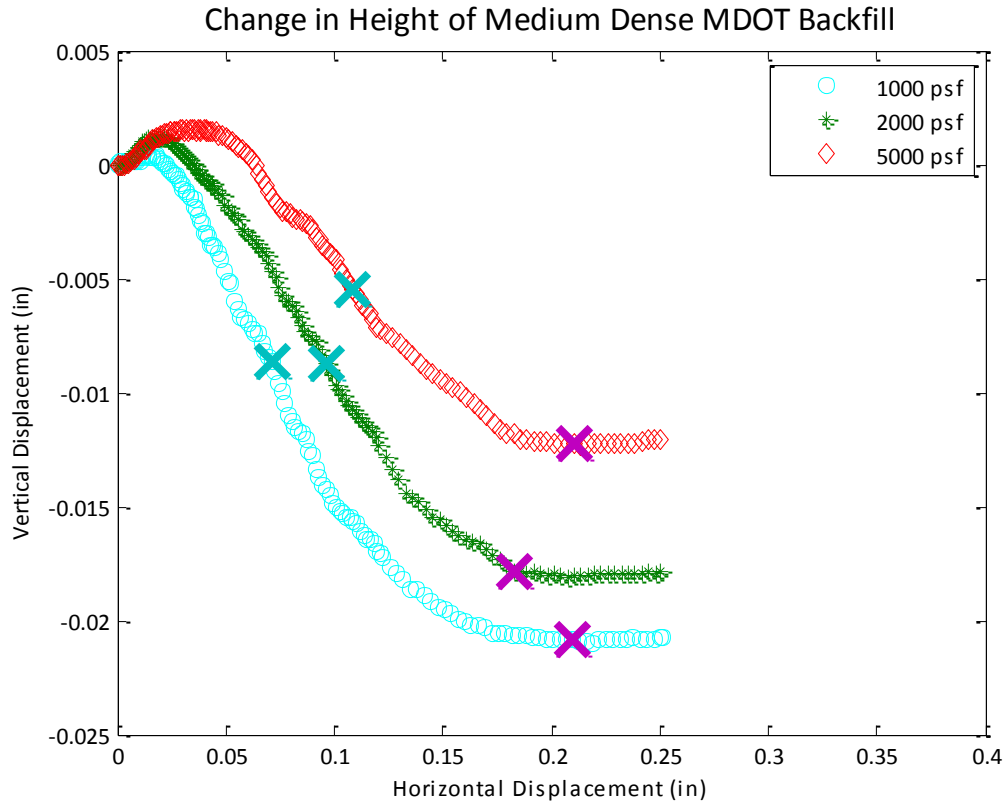
Direct Shear Results



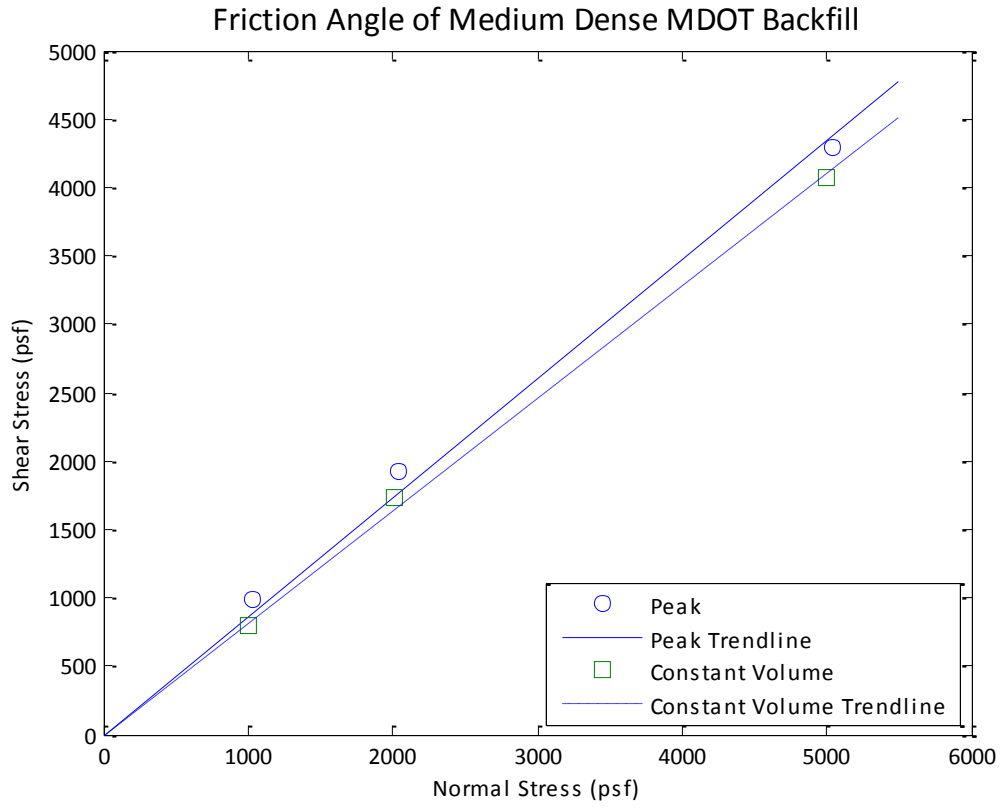
Direct Shear Results



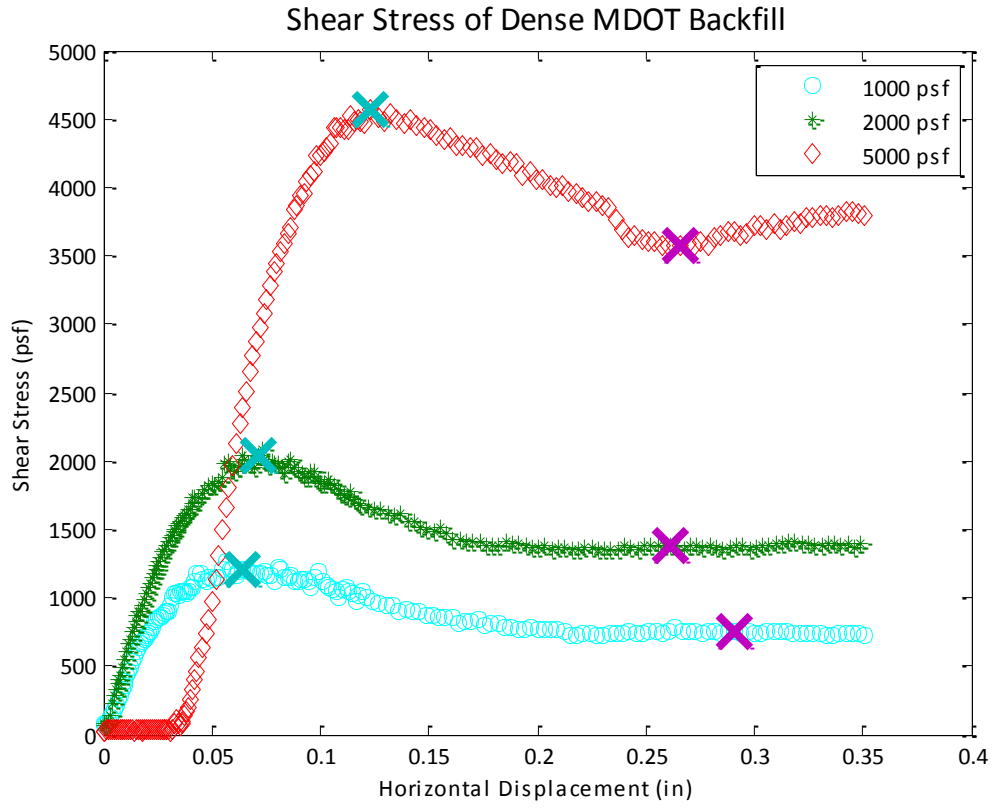
Direct Shear Results



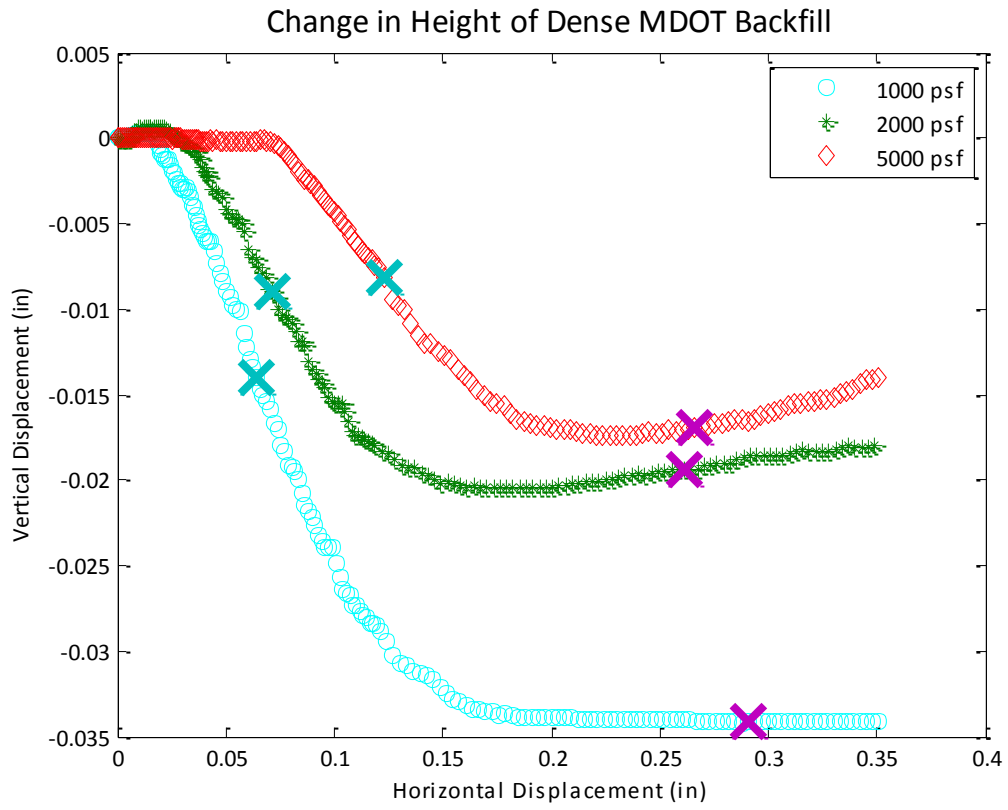
Direct Shear Results



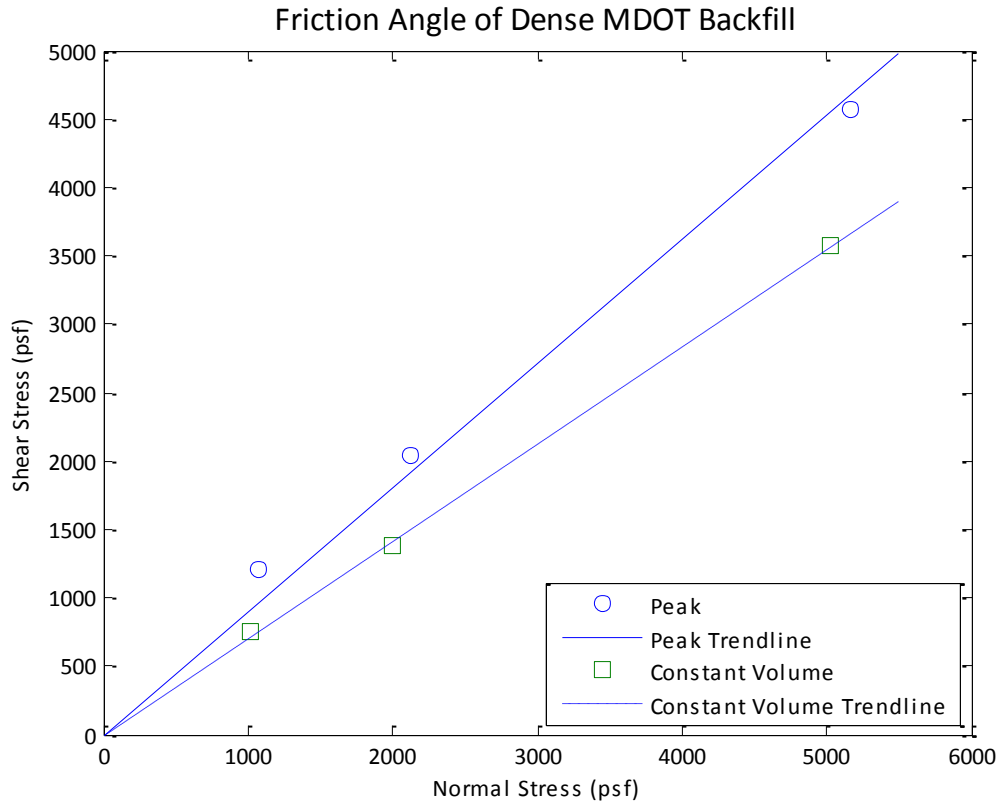
Direct Shear Results



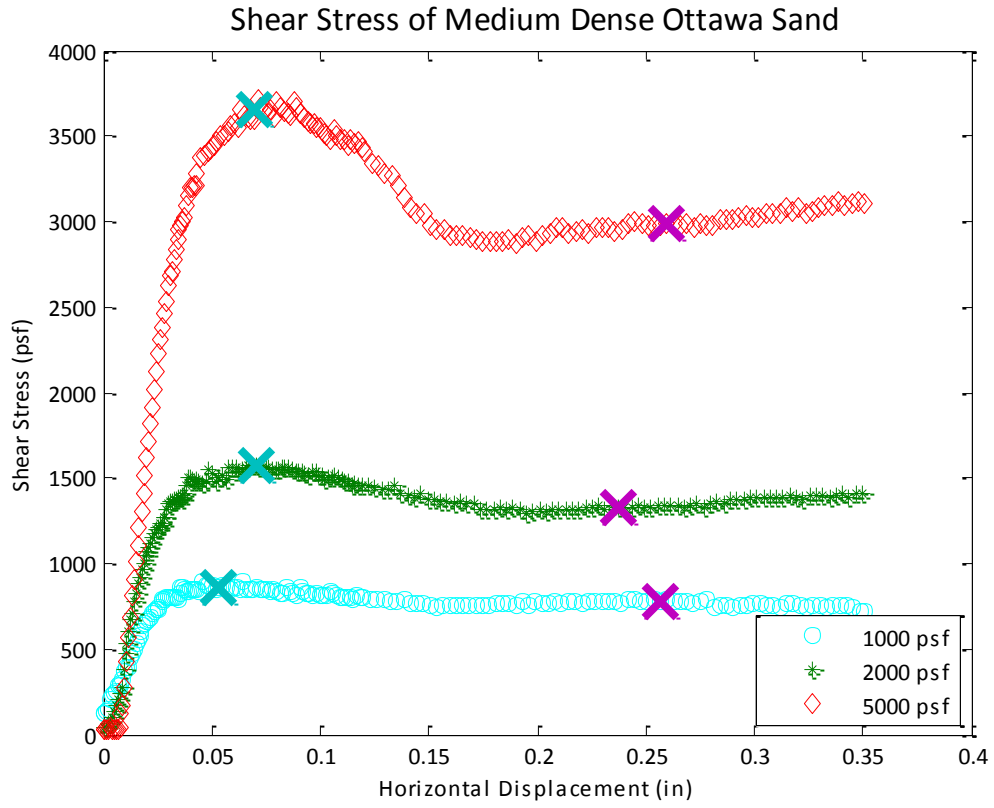
Direct Shear Results



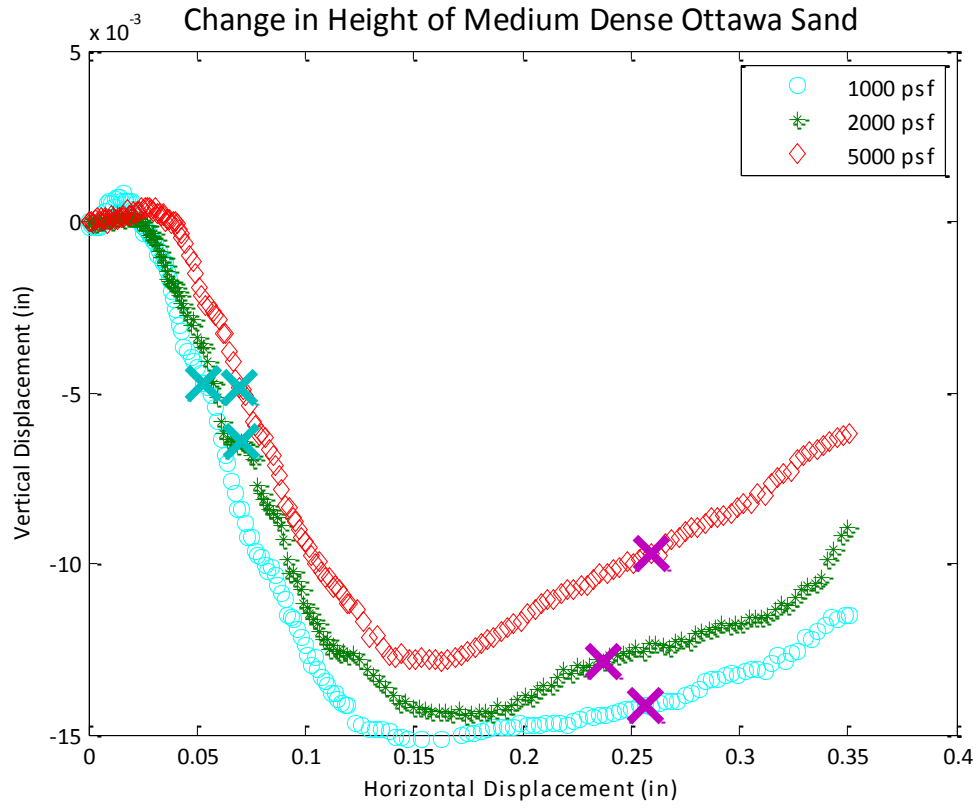
Direct Shear Results



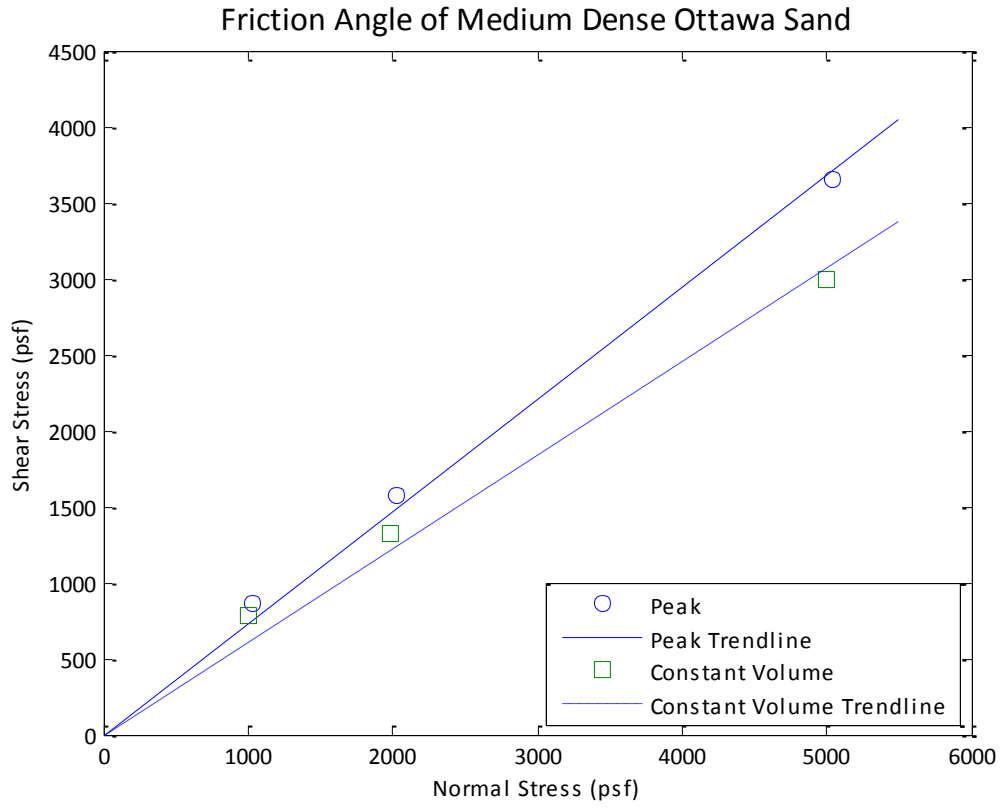
Direct Shear Results



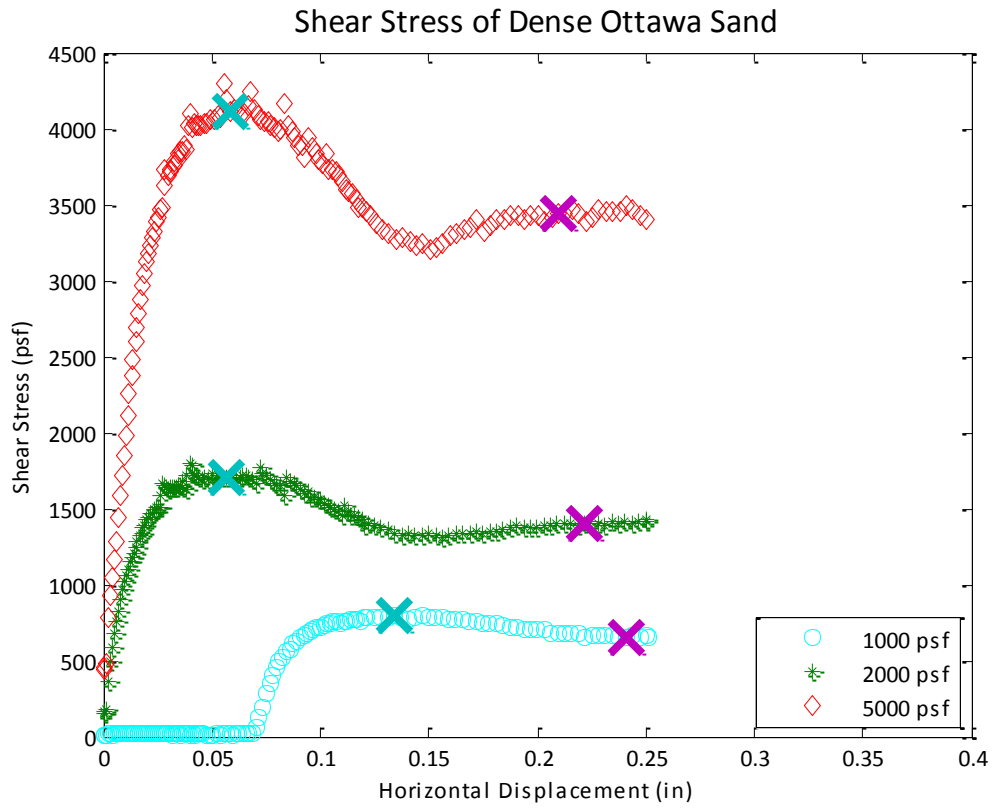
Direct Shear Results



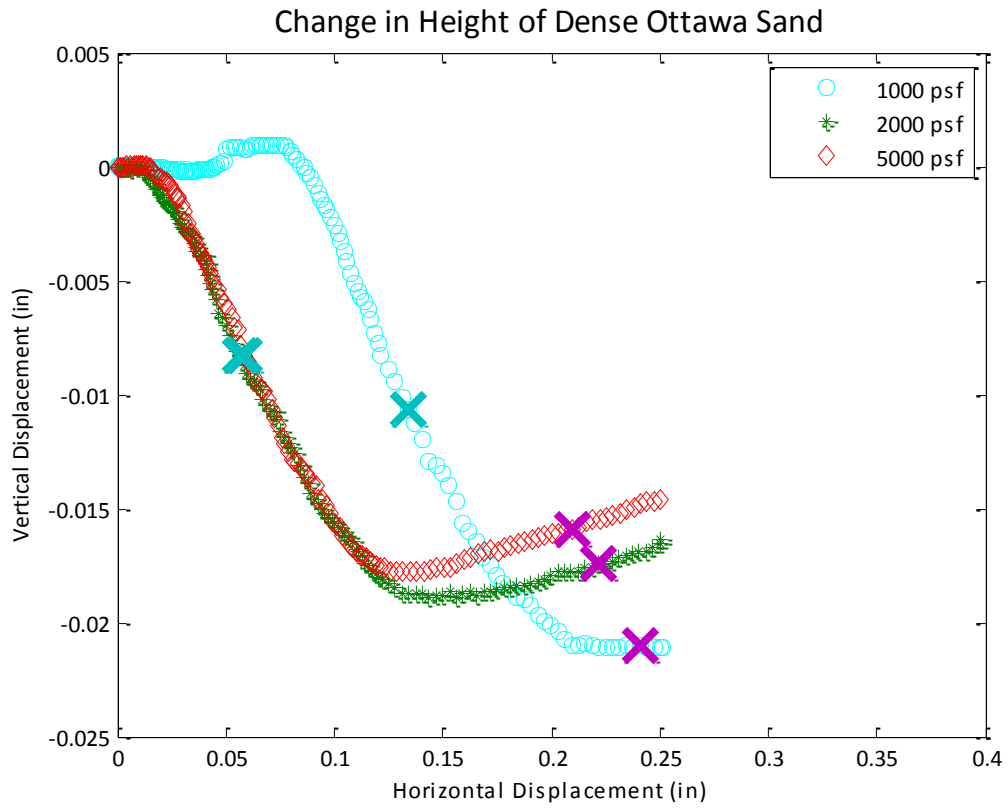
Direct Shear Results



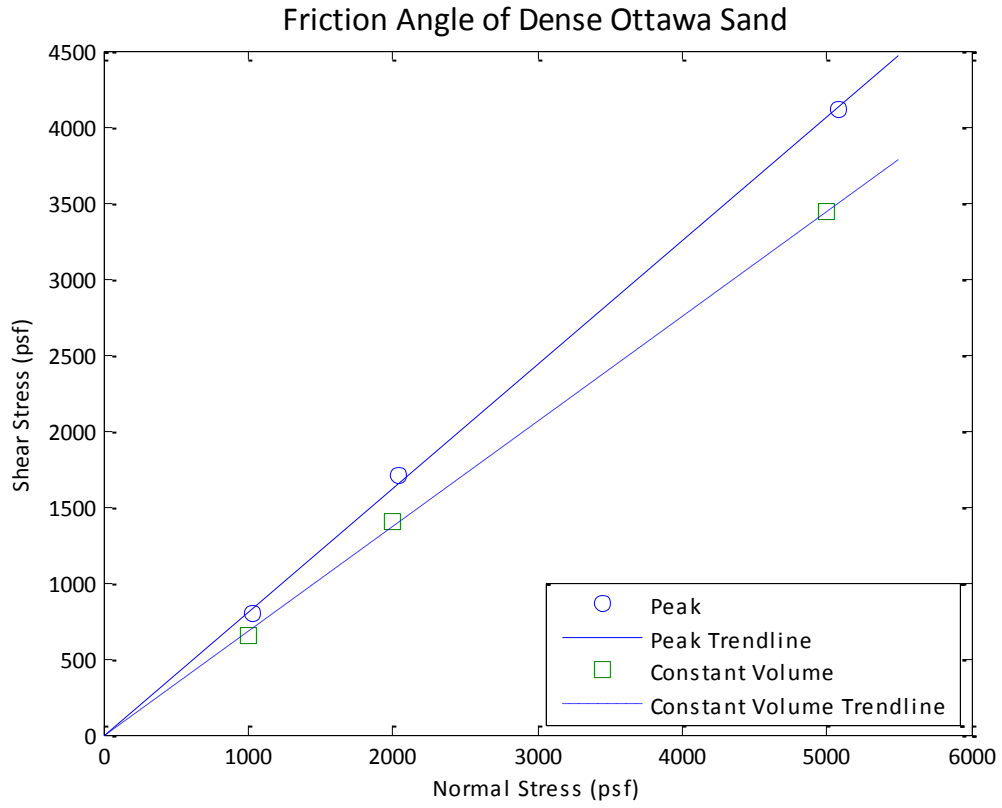
Direct Shear Results



Direct Shear Results

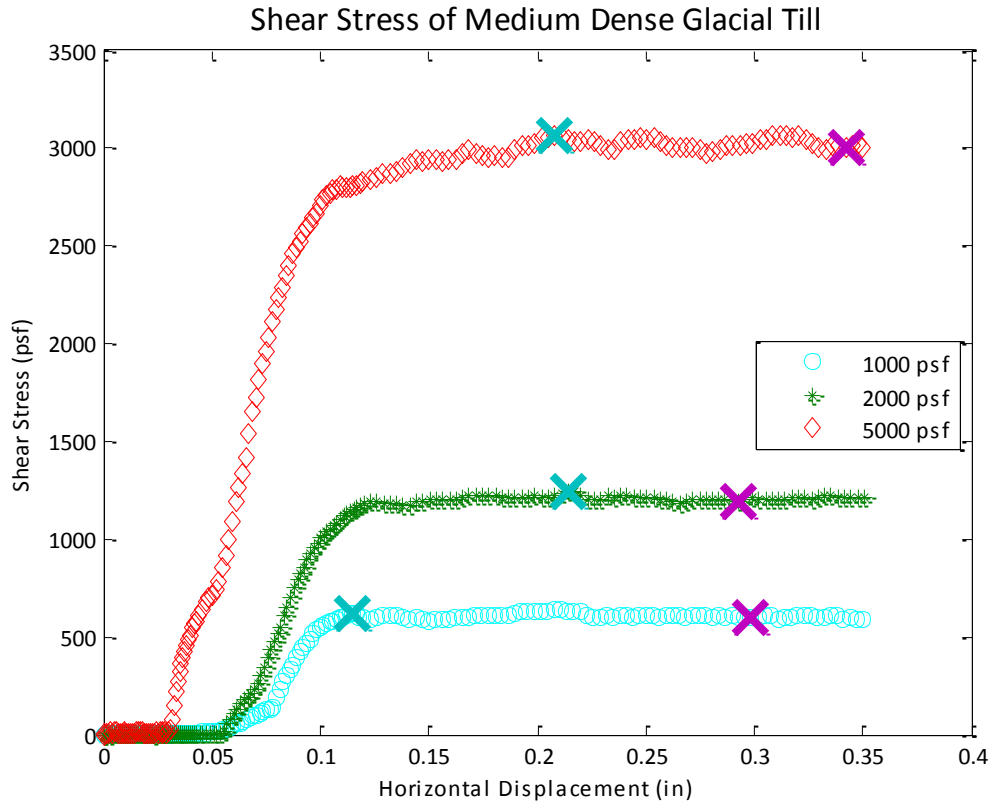


Direct Shear Results

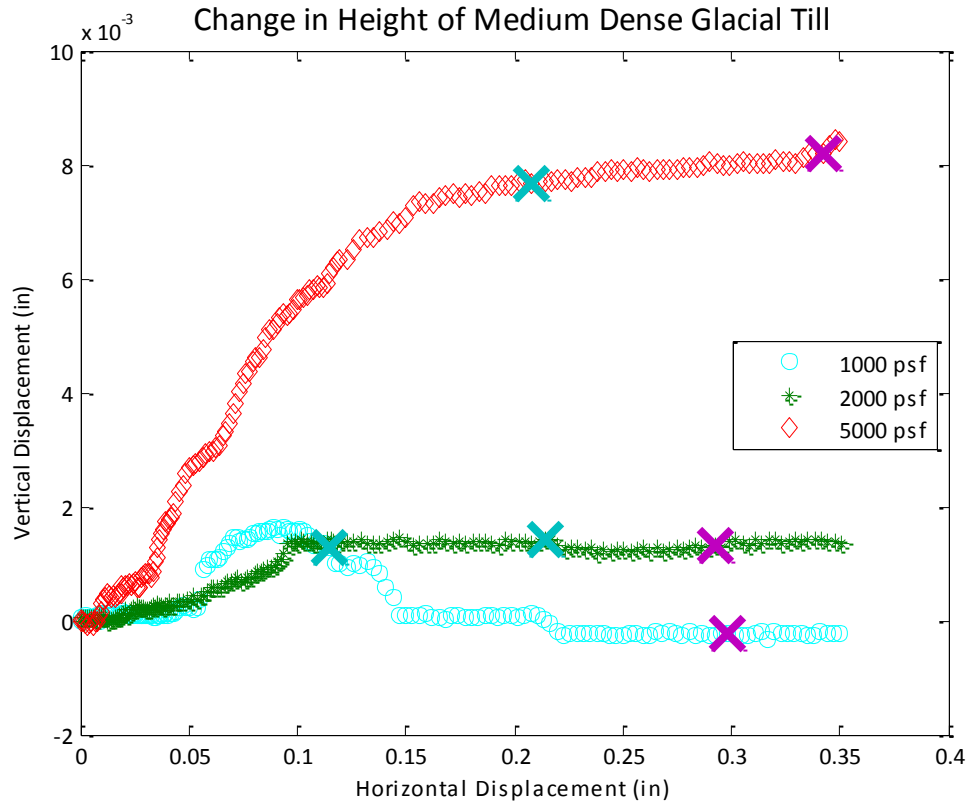


Appendix F: Interface Friction Results

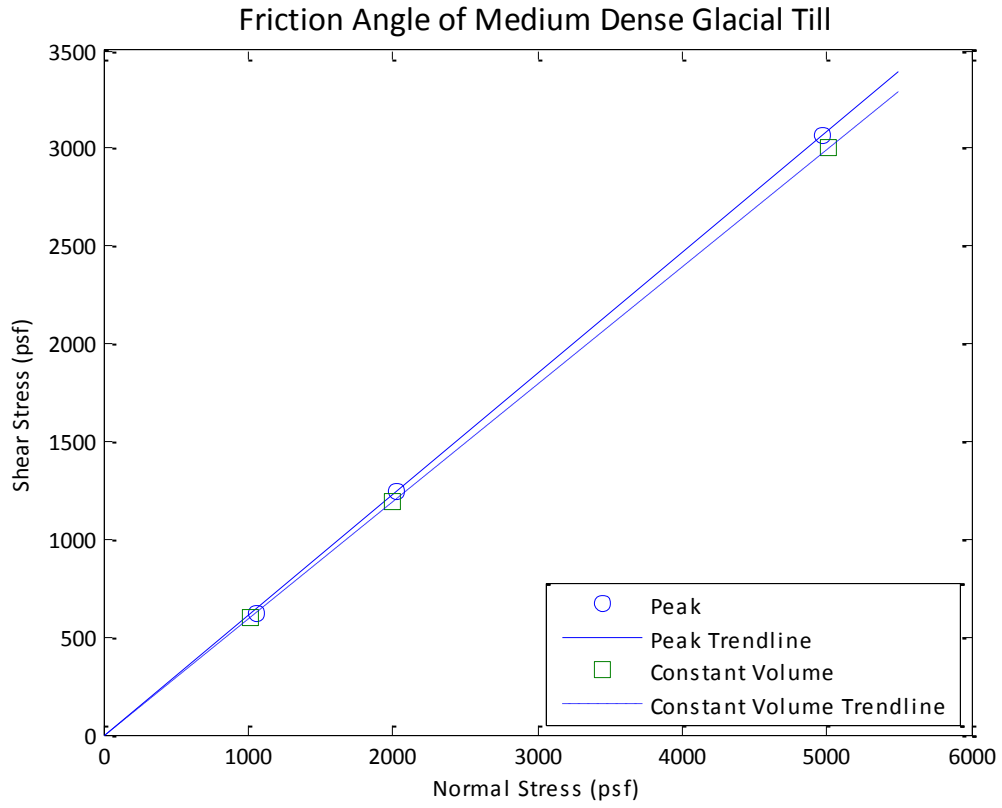
Interface Friction Results



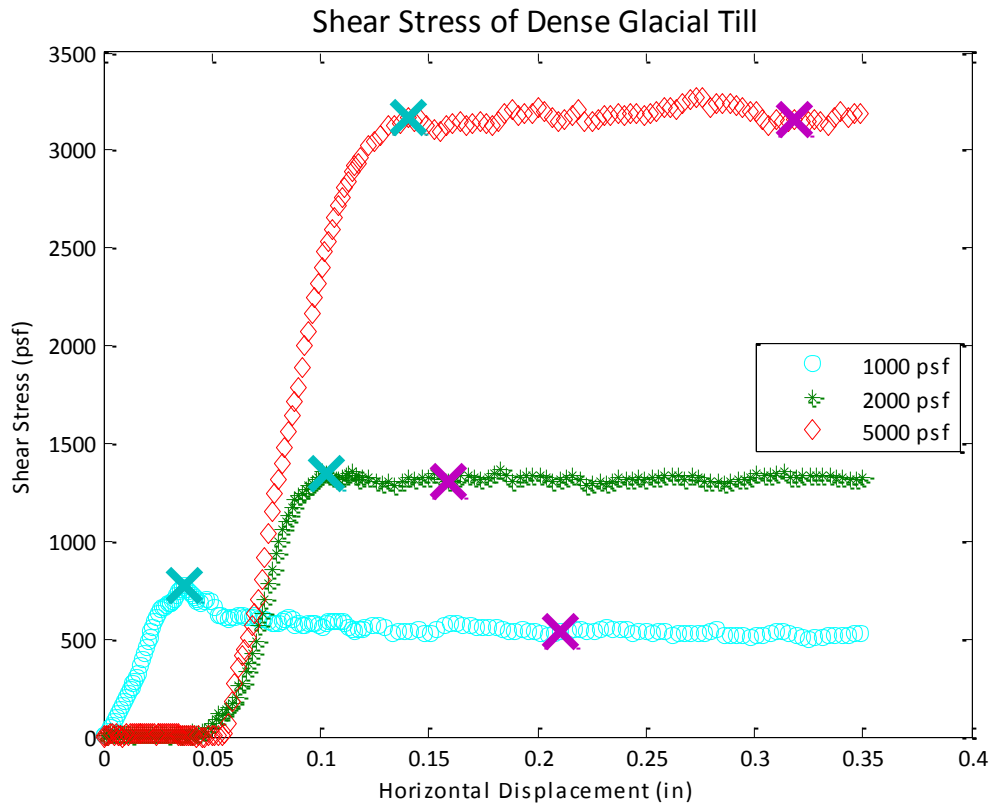
Interface Friction Results



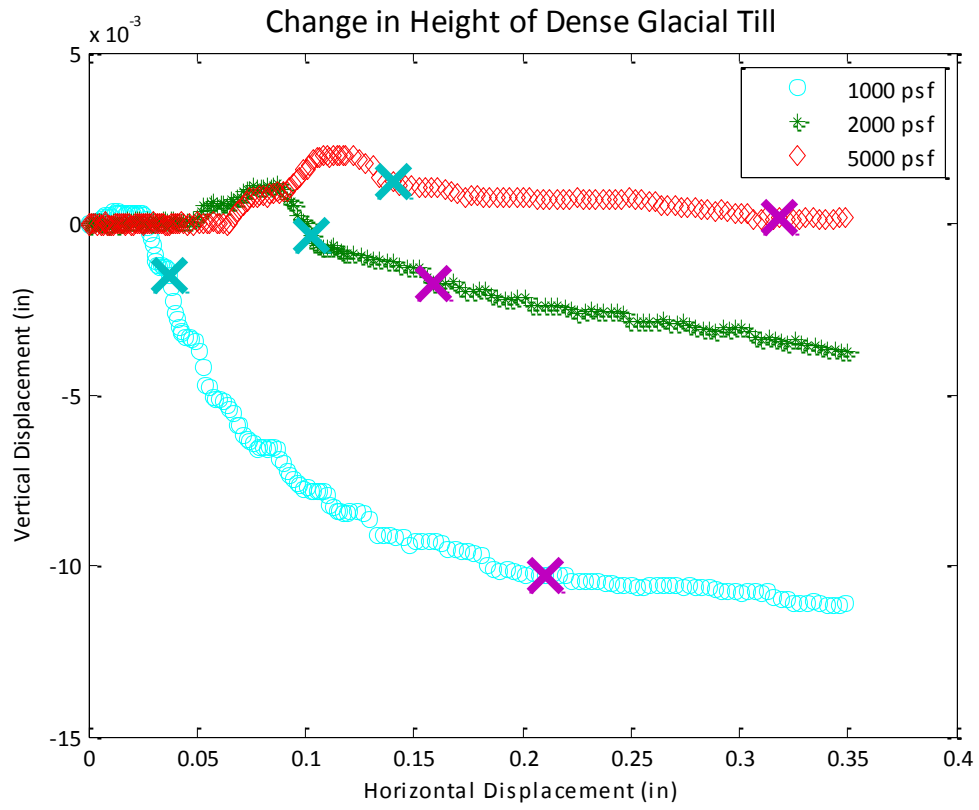
Interface Friction Results



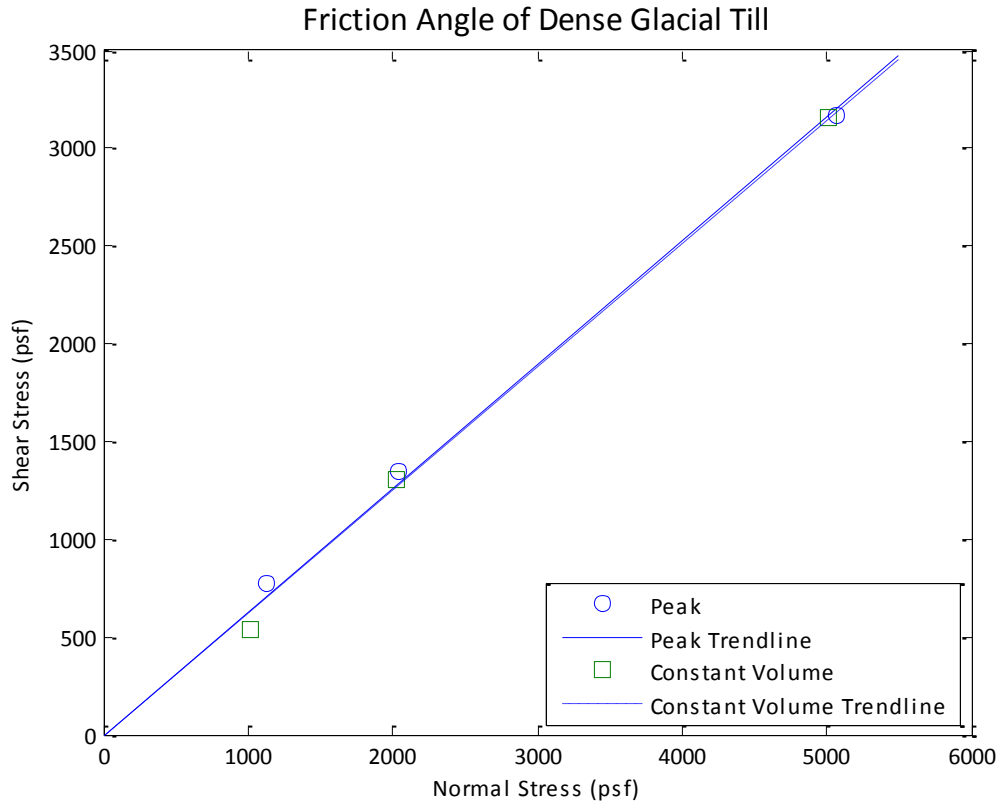
Interface Friction Results



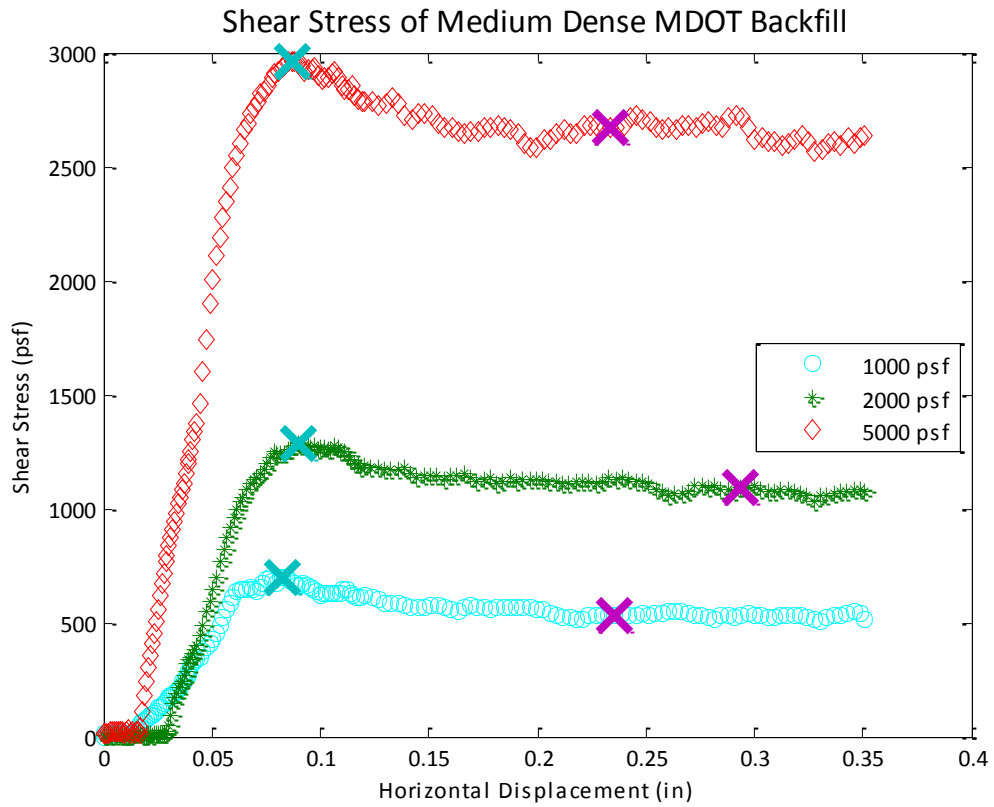
Interface Friction Results



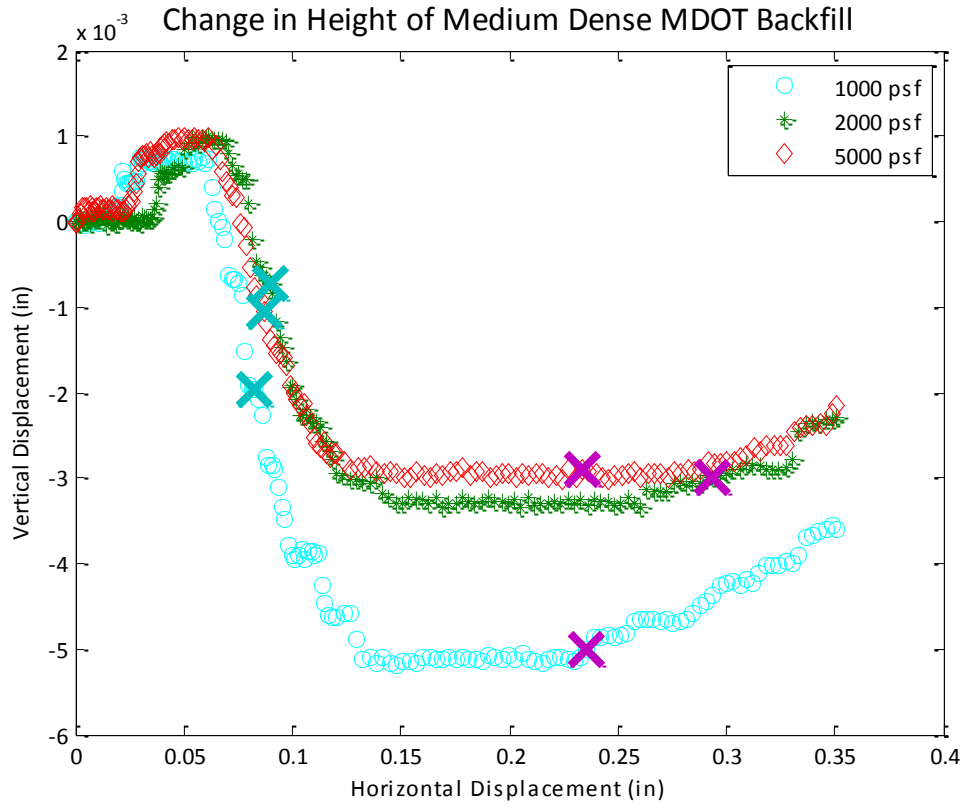
Interface Friction Results



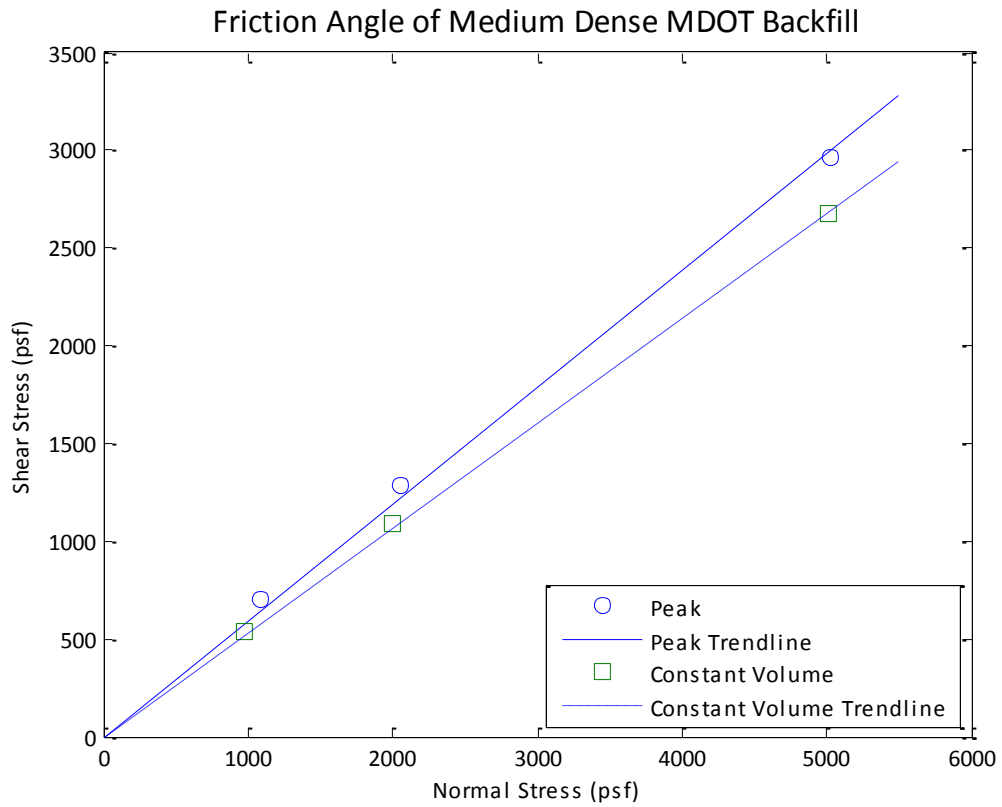
Interface Friction Results



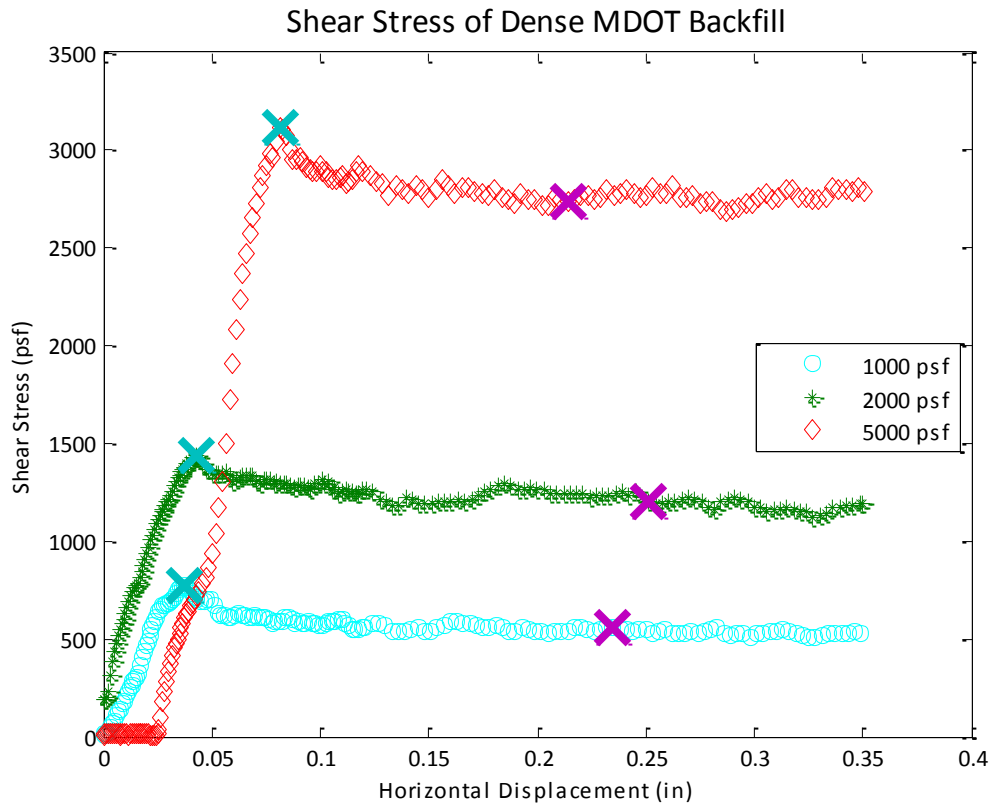
Interface Friction Results



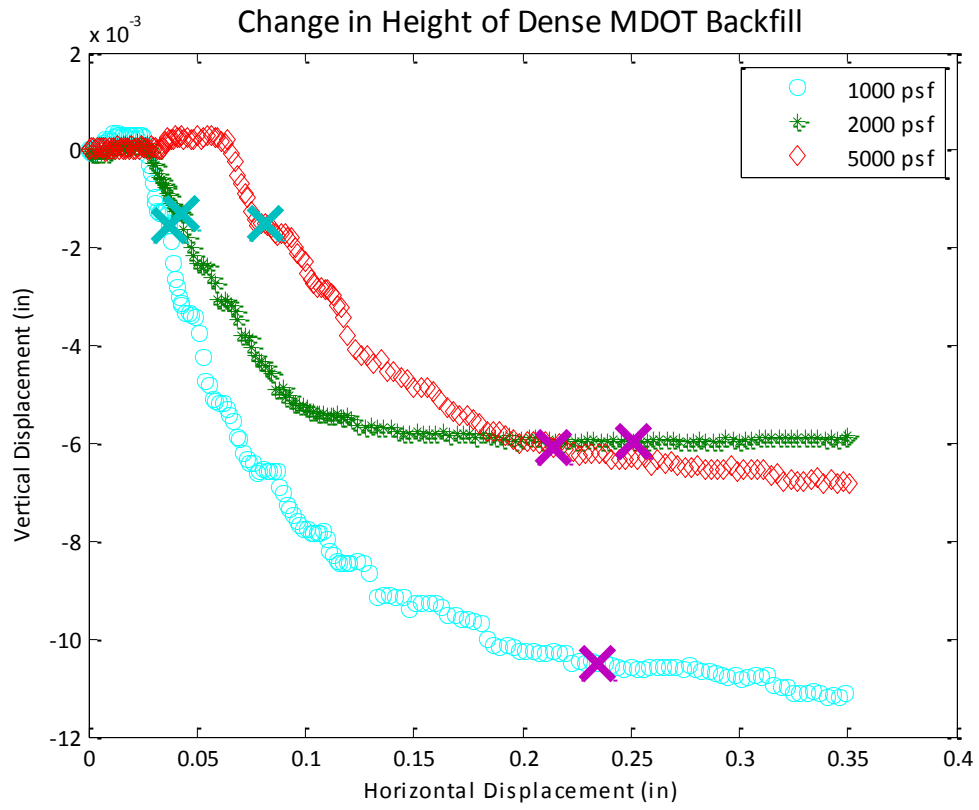
Interface Friction Results



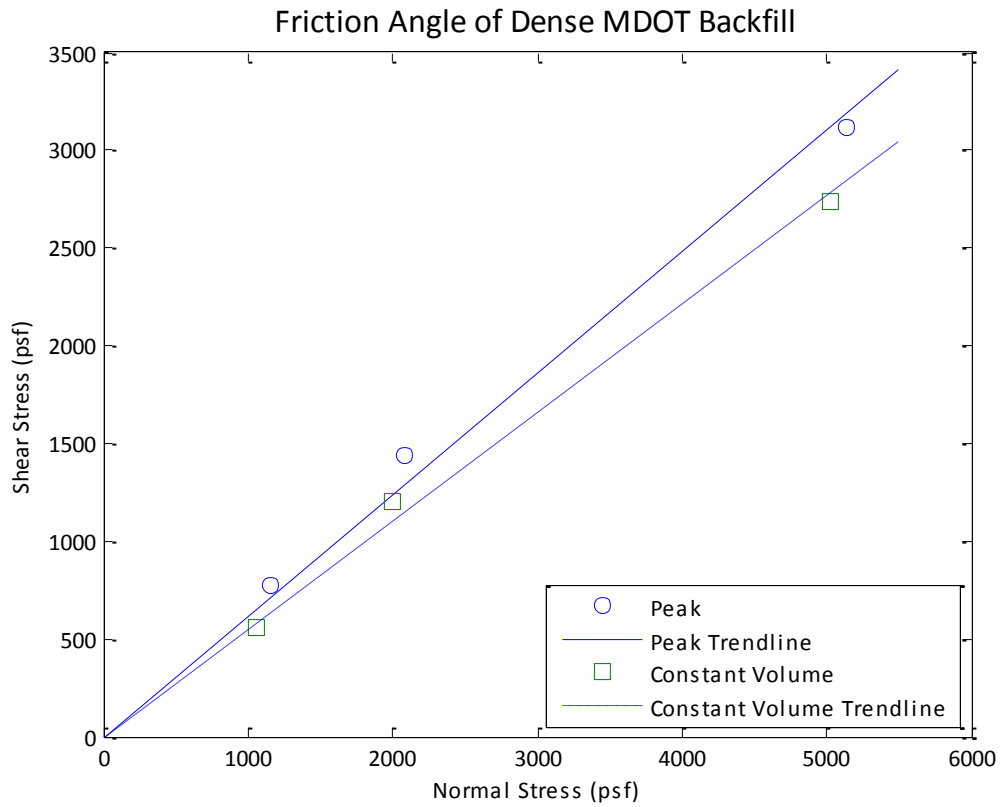
Interface Friction Results



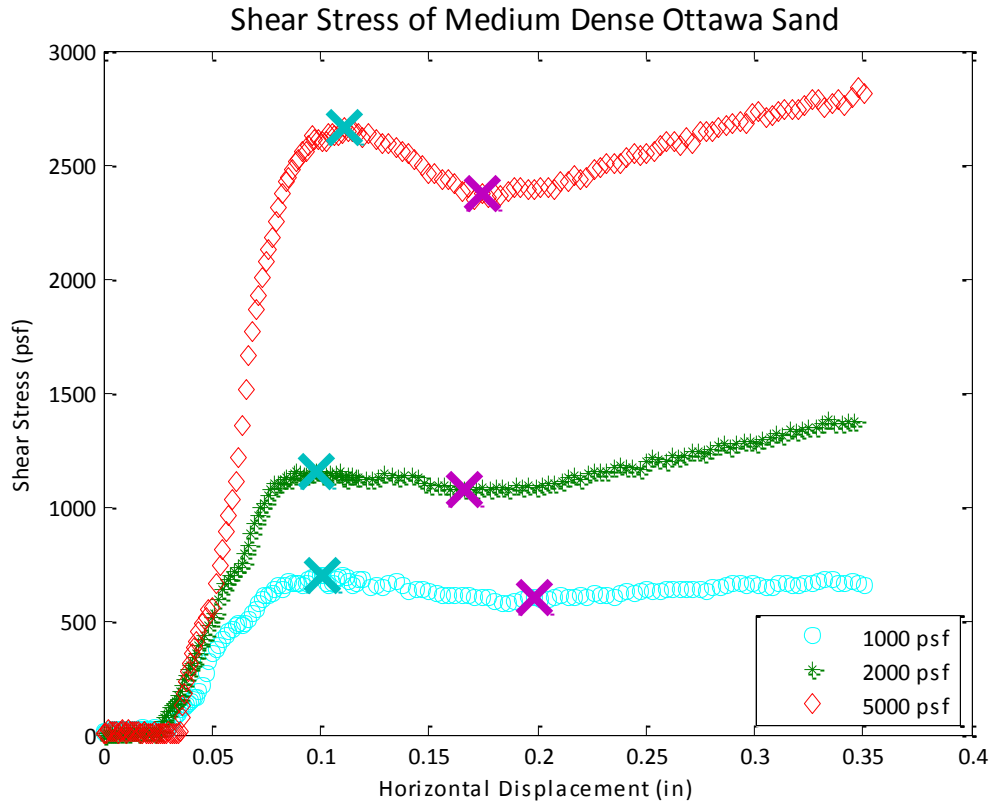
Interface Friction Results



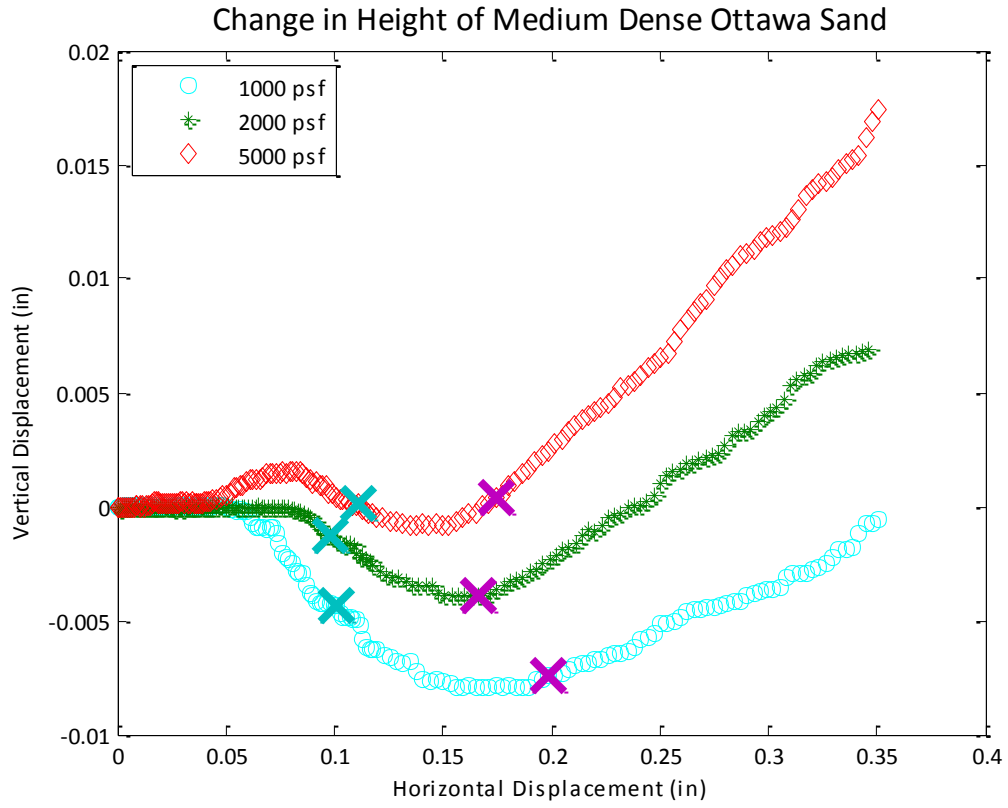
Interface Friction Results



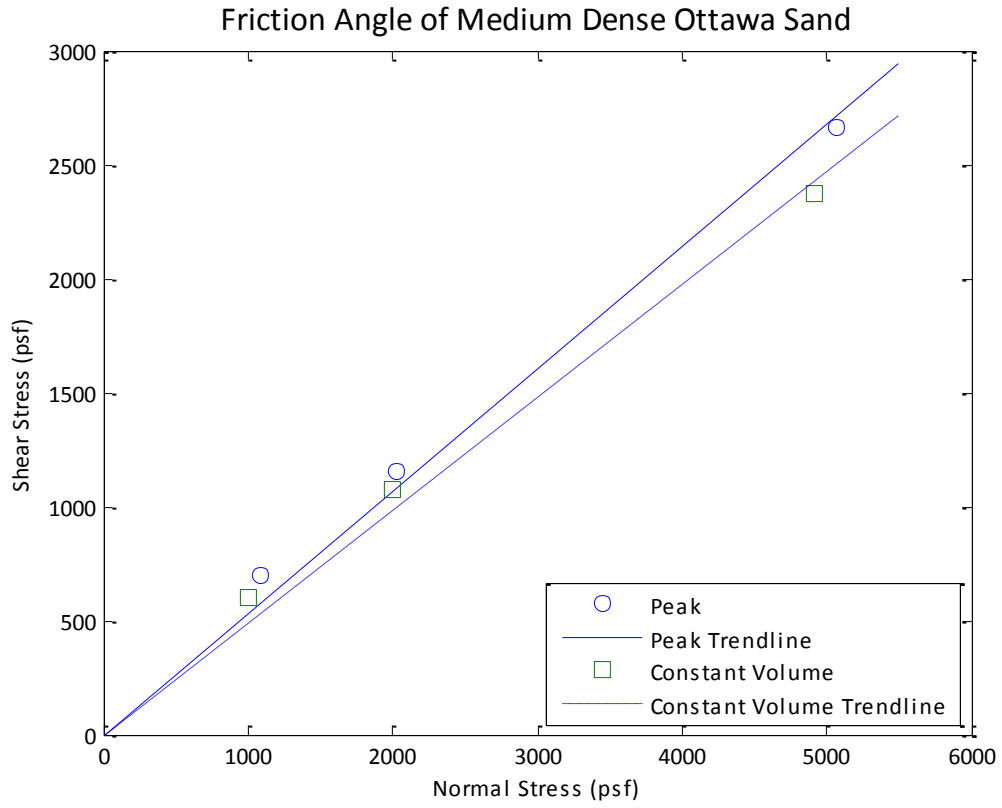
Interface Friction Results



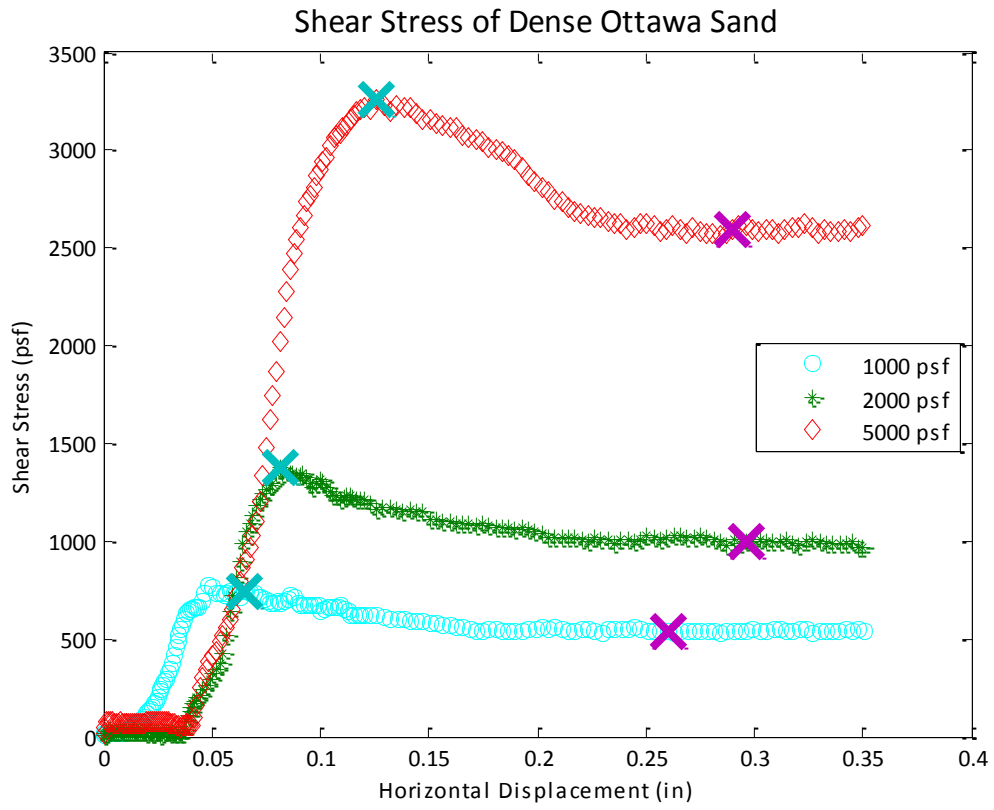
Interface Friction Results



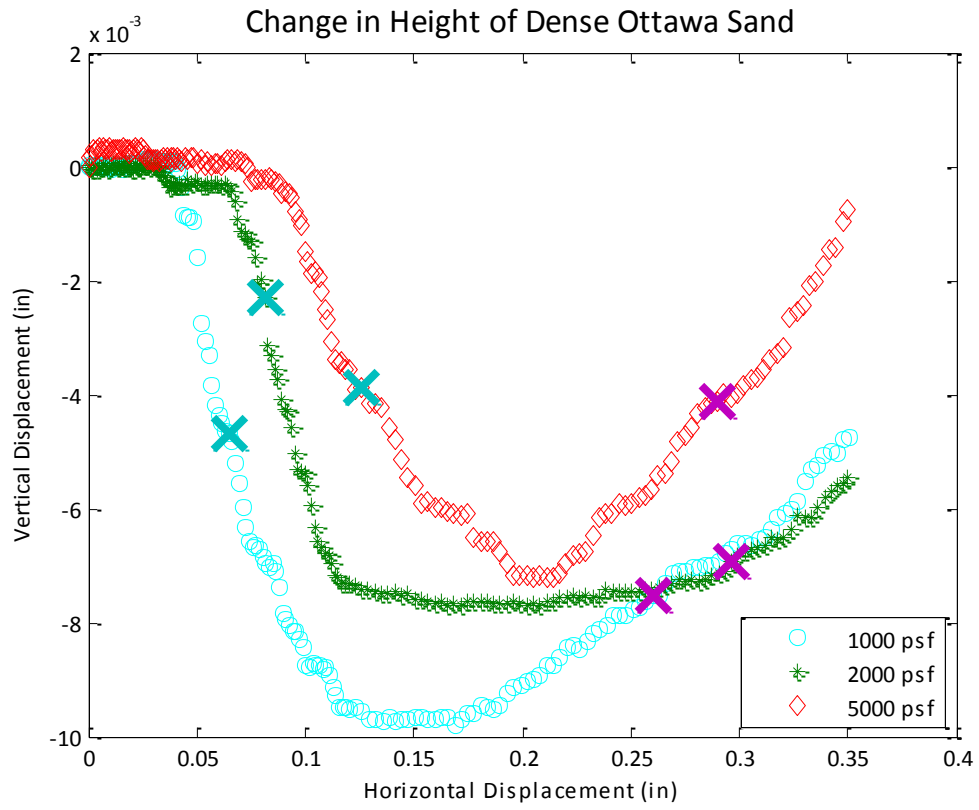
Interface Friction Results



Interface Friction Results



Interface Friction Results



Interface Friction Results

